nature human behaviour

ARTICLES

PUBLISHED: 24 APRIL 2017 | VOLUME: 1 | ARTICLE NUMBER: 0069

Evidence for a large-scale brain system supporting allostasis and interoception in humans

Ian R. Kleckner[1]*, Jiahe Zhang[1], Alexandra Touroutoglou[2,3,4], Lorena Chanes[1,3,4], Chenjie Xia[3,5], W. Kyle Simmons[6,7], Karen S. Quigley[1,8], Bradford C. Dickerson[3,5†] and Lisa Feldman Barrett[1,3,4*†]

Large-scale intrinsic brain systems have been identified for exteroceptive senses (such as sight, hearing and touch). We introduce an analogous system for representing sensations from within the body, called interoception, and demonstrate its relation to regulating peripheral systems in the body, called allostasis. Employing the recently introduced Embodied Predictive Interoception Coding (EPIC) model, we used tract-tracing studies of macaque monkeys, followed by two intrinsic functional magnetic resonance imaging samples ($N = 280$ and $N = 270$) to evaluate the existence of an intrinsic allostatic–interoceptive system in the human brain. Another sample ($N = 41$) allowed us to evaluate the convergent validity of the hypothesized allostatic–interoceptive system by showing that individuals with stronger connectivity between system hubs performed better on an implicit index of interoceptive ability related to autonomic fluctuations. Implications include insights for the brain's functional architecture, dissolving the artificial boundary between mind and body, and unifying mental and physical illness.

The brain contains intrinsic systems for processing exteroceptive sensory inputs from the world, such as vision, audition and proprioception/touch[1]. Accumulating evidence indicates that these systems work via the principles of predictive coding[2–7], in which sensations are anticipated and then corrected by sensory inputs from the world. The brain, as a generative system, models the world by predicting, rather than reacting to, sensory inputs. Predictions guide action and perception by continually constructing possible representations of the immediate future based on their prior probabilities relative to the present context[8,9]. We and others have recently begun to study the hypothesis that ascending sensory inputs from the organs and systems within the body's internal milieu are similarly anticipated and represented (autonomic visceral and vascular function, neuroendocrine fluctuations and neuroimmune function)[10–16]. These sensations are referred to as interoception[17–19]. Engineering studies of neural design[20], along with physiological evidence[21], indicate that the brain continually anticipates the body's energy needs in an efficient manner and prepares to meet those needs before they arise (for example, physical movements to cool the body's temperature before it gets too hot). This process is called allostasis[20–22]. Allostasis is not a condition or state of the body — it is the process by which the brain efficiently maintains energy regulation in the body. Allostasis is defined in terms of prediction, and recent theories propose that the prediction of interoceptive signals is necessary for successful allostasis[10,15,23–25]. Thus, in addition to the ascending pathways and brain regions important for interoception[17,18,26,27], recent theoretical discussions[11] have proposed the existence of a distributed intrinsic allostatic–interoceptive system in the brain (analogous to the exteroceptive systems). A full investigation of the predictive nature of an allostatic–interoceptive brain system requires multiple studies under various conditions. Here, we identify the anatomical and functional substrates for a unified allostatic–interoceptive system in the human brain and report an association between connectivity within this system and individual differences in interoceptive-related behaviour during allostatically relevant events.

We first review tract-tracing studies of non-human animals that provide the anatomical substrate for our hypothesis that the brain contains a unified, intrinsic system for allostasis and interoception. Next, we present evidence of this hypothesized system in humans using functional connectivity analyses on three samples of task-independent ('resting state') functional magnetic resonance imaging (fMRI) data (also called 'intrinsic' connectivity). We then present brain–behaviour evidence to validate the hypothesized allostatic–interoceptive system by using an implicit measure of interoception during an allostatically challenging task. Finally, we summarize empirical evidence to show that this allostatic–interoceptive system is a domain-general system that supports a wide range of psychological functions including interoception, emotion, memory, reward and cognitive control[28,29]. That is, whatever else this system might be doing — remembering, directing attention and so on — it is also predictively regulating the body's physiological systems in the service of allostasis to achieve those functions[23].

Our work synthesizes anatomical and functional brain studies that together provide evidence of a single brain system — comprising the salience and default mode networks — that supports not just allostasis but a wide range of psychological functions (such as emotion, pain, memory and decision-making) that can all be explained by their reliance on allostasis. To our knowledge, this evidence and our simple yet powerful explanation has not been presented despite the fact that many functional imaging studies show that the salience and default mode networks support a wide range of

[1]Department of Psychology, Northeastern University, 105–107 Forsyth Street, Boston, Massachusetts 02115, USA. [2]Department of Neurology, Massachusetts General Hospital and Harvard Medical School, 15 Parkman Street, Boston, Massachusetts 02114, USA. [3]Athinoula A. Martinos Center for Biomedical Imaging, 149 13th Street, Charlestown, Massachusetts 02129, USA. [4]Psychiatric Neuroimaging Division, Department of Psychiatry, Massachusetts General Hospital and Harvard Medical School, 55 Fruit Street Boston, Massachusetts 02114, USA. [5]Frontotemporal Disorders Unit, Department of Neurology, Massachusetts General Hospital and Harvard Medical School, 55 Fruit Street Boston, Massachusetts 02114, USA. [6]Laureate Institute for Brain Research, 6655 South Yale Avenue, Tulsa, Oklahoma 74136, USA. [7]School of Community Medicine, The University of Tulsa, 4502 East 41st Street, Tulsa, Oklahoma 74135, USA. [8]Edith Nourse Rogers Memorial VA Hospital, 200 Springs Road, Bedford, Massachusetts 01730, USA. †These authors jointly supervised this work. *e-mail: ian_kleckner@urmc.rochester.edu; l.barrett@neu.edu

© 2017 Macmillan Publishers Limited, part of Springer Nature. All rights reserved.

Table 1 | Summary of this study's hypotheses, predictions or questions, and results.

EPIC hypothesis	Experimental prediction	Result in the current study
Interoception and visceromotor control are part of a unified brain system that supports allostasis (Fig. 1).	Primary interoceptive cortex (for example, dmIns/dpIns) is anatomically and functionally connected to agranular and dysgranular visceromotor hubs of the cortex (for example, sgACC, pACC, aMCC).	The interoceptive and visceromotor hubs are anatomically connected in monkeys (Table 2). The interoception and visceromotor hubs are functionally connected in humans (Fig. 2, Supplementary Table 1). Coordinates for human hubs are shown in Table 3.
	The allostatic–interoceptive system also includes subcortical and brainstem visceromotor regions.	Previously established subcortical and brainstem visceromotor regions (for example, hypothalamus and PAG) are part of the unified system for allostasis/interoception (Fig. 4, Supplementary Fig. 6).
	The allostatic–interoceptive brain system contains limbic cortices.	The allostatic–interoceptive system comprises two established large-scale brain networks that contain the majority of limbic cortices: the salience network and the default mode networks (Fig. 3, Supplementary Fig. 3).
	Connectivity in the allostatic–interoceptive system is related to an implicit performance measure of interoception in humans.	The correspondence between sympathetic arousal (electrodermal activity) and experienced arousal during an allostatically challenging task is related to functional connectivity within the allostatic–interoceptive system in humans (Supplementary Fig. 8).
The allostatic–interoceptive system is domain-general.	The allostatic–interoceptive system sits at the core of the brain's computational architecture.	Many hubs of the allostatic–interoceptive system have been previously identified as members of the 'rich club', which are the most densely connected within the brain and therefore help to constitute the brain's 'neural backbone' for coordinating neural synchrony (Fig. 3, Supplementary Table 4).
	Brain activity and connectivity in the allostatic–interoceptive system is associated with a variety of psychological functions.	Both the default mode network and the salience network support various mental phenomena across major psychological domains (for example, cognition, emotion, perception and action; Fig. 5).

Other hypotheses, such as the computational dynamics of the proposed allostatic–interoceptive network, are beyond the scope of this study. pACC, pregenual anterior cingulate cortex.

psychological functions (that is, they are domain-general[30]; see previous reviews[28,29]). Our paper provides the groundwork for a theoretical and empirical framework for making sense of these findings in an anatomically principled way. Our key hypotheses and results are summarized in Table 1.

Anatomical evidence supporting the proposed allostatic–interoceptive system

Over three decades of tract-tracing studies of the macaque monkey brain clearly demonstrate an anatomical substrate for the proposed flow of the brain's prediction and prediction error signals. Specifically, anatomical studies indicate a flow of information within the laminar gradients of these cortical regions according to the structural model of corticocortical connections in ref. [31] (for a review, see ref. [32]). In addition, this structural model of corticocortical connections has been seamlessly integrated with a predictive coding framework[11,12]. Unlike other models of information flow that work in specific regions of cortex, the structural model successfully predicts information flow in frontal, temporal, parietal and occipital cortices[33–37]. Accordingly, prediction signals flow from regions with less laminar development (for example agranular regions) to regions with greater laminar development (for example granular regions), whereas prediction error signals flow in the other direction.

In our recently developed theory of interoception, the EPIC model[11], we integrated the active inference approach to predictive coding[38–40] with the structural model of ref. [31] to hypothesize that less-differentiated agranular and dysgranular visceromotor cortices in the cingulate cortex and anterior insula initiate visceromotor predictions through their cascading connections to the hypothalamus, the periaqueductal grey (PAG) and other brainstem nuclei known to control the body's internal milieu[41–44] (also see ref. [32]; red pathways in Fig. 1); simultaneously, the cingulate cortex and anterior insula send the anticipated sensory consequences of those visceromotor actions (that is, interoceptive predictions) to the more granular primary interoceptive cortex in the dorsal mid to posterior insula (dmIns/dpIns[18,45,46]; blue solid pathways in Fig. 1). Using this logic, we identified a key set of cortical regions with visceromotor connections that should form the basis of our unified system for interoception and allostasis (we also included one subcortical region, the dorsal amygdala (dAmy), in this analysis because of the role of the central nucleus in visceromotor regulation; see Methods for details). This evidence is summarized in Table 2. As predicted by our EPIC model, most of the key visceromotor regions in the proposed interoceptive system do, in fact, have monosynaptic, bidirectional connections to primary interoceptive cortex, reinforcing the hypothesis that they directly exchange interoceptive prediction and prediction error signals. We also confirmed that these visceromotor cortical regions do indeed monosynaptically project to the subcortical and brainstem regions that control the internal milieu (that is, the autonomic nervous system, immune system and neuroendocrine system), such as the hypothalamus, PAG, parabrachial nucleus (PBN), ventral striatum, and nucleus of the solitary tract (NTS) (Table 2, right column).

Next, we tested for evidence of these connections in functional data from human brains. Axonal connections between neurons, both direct (monosynaptic) and indirect (for example, disynaptic) connections, are closely reflected in intrinsic brain systems (see previous reviews[47,48]). As such, we tested for evidence of these connections in functional connectivity analyses on two samples of low-frequency, blood oxygenation-level dependent (BOLD) signals during task-independent (that is, 'resting state') fMRI scans collected on human participants (discovery sample, $N = 280$, 174 female, mean age = 19.3 years, s.d. = 1.4 years; replication sample, $N = 270$, 142 female, mean age = 22.3 years, s.d. = 2.1 years).

© 2017 Macmillan Publishers Limited, part of Springer Nature. All rights reserved.

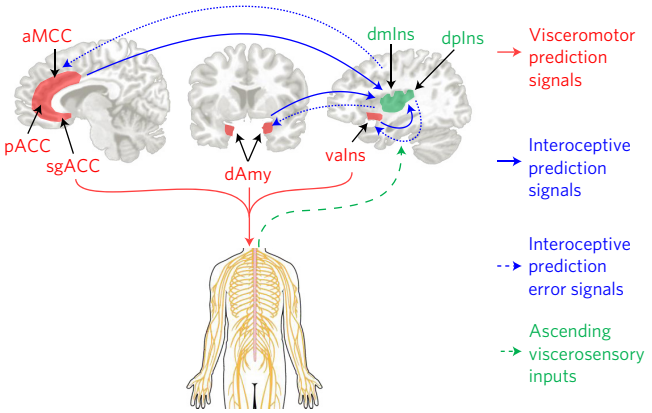

Figure 1 | We identified key visceromotor cortical regions (in red) that provide cortical control of the body's internal milieu. The regions include the aMCC (also called dorsal anterior cingulate cortex[41,42]), pregenual anterior cingulate cortex (pACC), sgACC (for a review of the cingulate, see ref. [176]) and the vaIns (also called agranular insula[43,183] or posterior orbitofrontal cortex[193]); these regions have a less-developed laminar structure (that is, they are agranular or dysgranular[32,176]). We also included the dAmy because it contains the central nucleus which is also involved in visceromotor control (for a review, see ref. [145]). Primary interoceptive cortex spans the dmIns to the dpIns[17] along a dysgranular to granular[194] gradient (green regions). Previous work[11] summarized preliminary tract-tracing evidence, supporting the EPIC model, demonstrating that allostasis and interoception are maintained within an integrated system involving limbic cortices (in red) that initiate visceromotor directions to the hypothalamus and brainstem nuclei (for example, PAG, PBN and NTS; citations in Table 2) to regulate the autonomic, neuroendocrine and immune systems (red paths). These visceromotor control regions (less-developed laminar organization) also send anticipated sensory consequences of visceromotor changes (as interoceptive prediction signals) to primary interoceptive cortex (more-developed laminar organization; solid blue paths). The incoming sensory inputs from the internal milieu of the body are carried along the vagus nerve and small-diameter C and Aδ fibres (dashed green path) to primary interoceptive cortex in the dorsal sector of the mid to posterior insula (for a review, see ref. [17]); comparisons between prediction signals and ascending sensory input results in interoceptive prediction error. Current interoceptive predictions can be updated by passing prediction error signals to visceromotor regions (dashed blue paths); prediction errors are learning signals and also adjust subsequent predictions. (For simplicity, ascending feedback to visceromotor regions is not shown.)

We then examined the validity of these connections in a third independent sample of participants ($N = 41$, 19 female, mean age = 33.5 years, s.d. = 14.1 years), following which we situated these findings in the larger literature on network function.

Results

Cortical and amygdalar intrinsic connectivity supporting a unified allostatic–interoceptive system in humans. Our seed-based approach estimated the functional connectivity between a set of voxels of interest (the seed) and the voxels in the rest of the brain as the correlation between the low-frequency portion of their BOLD signals over time, producing a discovery map for each seed region. Starting with the anatomical regions of interest specified by the EPIC model, and verified in the anatomical literature, we selected seed regions guided by previously published functional studies. We selected two groupings of voxels in primary interoceptive cortex (dpIns and dmIns) that consistently showed increased activity during task-dependent fMRI studies of interoception (Table 3, first and second rows). We selected seed regions for cortical visceromotor regions and the dAmy using related studies (Table 3, remaining rows). As predicted, the voxels in the primary interoceptive cortex and visceromotor cortices showed statistically significant intrinsic connectivity (Fig. 2; replication sample Supplementary Fig. 1). The dpIns was intrinsically connected to all visceromotor areas of interest (seven two-tailed, one-sample t-tests were each significant at $P < 10^{-7}$; Supplementary Table 1), and the dmIns was intrinsically connected to most of them (Supplementary Table 1). The discovery and replication samples demonstrated high reliability for connectivity profiles of all seeds (η^2 mean = 0.99, s.d. = 0.004).

Next, we computed η^2 for all pairs of maps to determine their spatial similarity[49] (mean = 0.56, s.d. = 0.17), and then performed k-means clustering of the η^2 similarity matrix to determine the configuration of the system. Results indicated that the allostatic–interoceptive system is composed of two intrinsic networks connected in a set of overlapping regions (Fig. 3; replication sample, Supplementary Fig. 2). The spatial topography of one network resembled an intrinsic network commonly known as the default mode network (Supplementary Figs 3 and 4; for a review, see ref. [50]). The second network resembled an intrinsic network commonly known as the salience network[51,52] (Supplementary Figs 3 and 4), the cingulo-opercular network[53] or the ventral attention network[54]. Resemblance was confirmed quantitatively by comparing the percentage overlap in our observed networks to reconstructions of the default mode and salience networks reported elsewhere[55] (Supplementary Table 2). Other cortical regions within the interoceptive system shown in Fig. 3 (for example, dorsomedial prefrontal cortex, middle frontal gyrus), not listed in Table 2, support visceromotor control by direct anatomical projections to the hypothalamus and PAG (Supplementary Table 3), supporting our hypothesis that this system plays a fundamental role in visceromotor control and allostasis.

Subcortical, hippocampal, brainstem and cerebellar connectivity supporting a unified allostatic–interoceptive system in humans. Using a similar analysis strategy, we assessed the intrinsic connectivity between the cortical and dorsal amygdalar seeds of interest and the thalamus, hypothalamus, cerebellum, the entire amygdala, hippocampus, ventral striatum, PAG, PBN and NTS. The observed functional connections with these cortical and amygdalar seeds, which regulate energy balance, strongly suggest that the proposed allostatic–interoceptive system itself also regulates energy balance (see Supplementary Discussion for details). All results replicated in our independent sample ($N = 270$; Supplementary Fig. 5, η^2 mean = 0.98, s.d. = 0.008). Figure 4 illustrates the connectivity between the default mode and salience networks and the non-cortical targets in the discovery sample. Supplementary Fig. 6 shows connectivity between the individual cortical and amygdalar seed regions listed in Table 2. We also observed specificity in the proposed allostasis/interoception system: non-visceromotor brain regions that are unimportant to interoception and allostasis, such as the superior parietal lobule (Supplementary Fig. 7), did not show functional connectivity to the subcortical regions of interest.

The cortical hubs of the allostatic–interoceptive system also overlapped in their connectivity to non-cortical regions involved in allostasis (purple in Fig. 4), including the dAmy, the hypothalamus, the PBN and two thalamic nuclei — the ventromedial posterior nucleus, and both the medial and lateral sectors of the mediodorsal nucleus (which shares strong reciprocal connections with medial and orbital sectors of the frontal cortex, the lateral sector of the amygdala, and other parts of the basal forebrain; for a review, see ref. [56]). Additionally, the connector hubs shared projections in the cerebellum and hippocampus (see Fig. 4).

Taken together, our intrinsic connectivity analyses failed to confirm only five monosynaptic connections (8%) that were predicted

© 2017 Macmillan Publishers Limited, part of Springer Nature. All rights reserved.

Table 2 | Summary of tract-tracing study results in non-human animals, demonstrating anatomical connections between cortical visceromotor and primary interoceptive sensory regions, as well as between cortical and non-cortical visceromotor regions

	Primary interoceptive cortex	Visceromotor regions				Subcortical and brainstem visceromotor structures	
	To dpIns/dmIns	**To vaIns**	**To sgACC (BA 25)**	**To pACC (BA 24, 32)**	**To aMCC (BA 24)**	**To amygdala**	**To other subcortical and brainstem regions***
From dpIns/dmIns	–	Case A, Fig. 1 of ref. [146]	Not evident†	Case 1, Fig. 5 of ref. [156]	Case B, Fig. 3 of ref. [157]	Case 2, Fig. 3 of ref. [147] Case BB-B, Fig. 1 of ref. [60]	Hypothalamus (rat)[158] PAG: not observed[159] PBN (rat)[160,161] Ventral striatum [162] NTS (rat)[161]
From vaIns‡	Case C, Fig. 4 of ref. [146] Case A, Fig. 1 of ref. [157]	-	Case OM20, Fig. 8 of ref. [163]	Case 1, Fig. 5 of ref. [156]	Case 2, Fig 6 of ref. [156] Case A, Fig. 1 of ref. [157]	Case A, Fig. 1 of ref. [157] Case 103, Fig. 3 of ref. [164] Fig. 2, Table 2 of ref. [165]	Hypothalamus[43] PAG[159] PBN (rat)[160] Ventral striatum[166] NTS (rat)[161]
From sgACC (BA 25)	Not evident§	Case M707[167]	–	Case 1, Fig. 5 of ref. [156] Fig. 2A of ref. [168]	Case 3, Fig. 7 of ref. [156] Fig. 3A of ref. [168]	Case 103, Fig. 3 of ref. [164] Fig. 5 of ref. [147]	Hypothalamus[147,169,170] PAG[159,170] PBN[170] Striatum[170] NTS (rat)[171,172]
From pACC (BA 24, 32)	Not evident§	Case M776[167]	Fig. 1 of ref. [168]	–	Case 3, Fig. 7 of ref. [156] Fig. 3A of ref. [168]	Case 103, Fig. 3 of ref. [164] Fig. 5 of ref. [147]	Hypothalamus[43] PAG[159] PBN (cat)[173] Ventral striatum (cat)[173] NTS (rat)[172]
From aMCC (BA 24)	Case C, Fig. 4 of ref. [146]	Case A, Fig. 1 of ref. [146]	Case 3, Fig. 4 of ref. [174]	Case 1, Fig. 5 of ref. [156] Fig. 2A of ref. [168]	–	Case 103, Fig. 3 of ref. [164] Fig. 5 of ref. [147]	Hypothalamus[43] PAG[159] PBN: not present[175] Ventral striatum[176] NTS (rat)[171]
From amygdala	Case C, Fig. 4 of ref. [146] Lateral basal nucleus, Case 5, Fig. 6 of ref. [147]	Case A, Fig. 1 of ref. [146] Case 4, Fig. 5 of ref. [147]	Fig. 6 of ref. [147]	Fig. 13 of ref. [168]	Fig. 6 of ref. [147]	–	Hypothalamus[43] PAG[159] PBN[177] Ventral striatum[178] NTS[177]

Note: connectivity evidence is in monkeys unless otherwise indicated (for example rats, cats). Some connections from dpIns/dmIns to the NTS are unclear, owing to ambiguity in how ref. [161] reported subregions of the insula.

*We did not assess projections from subcortical and brainstem regions to cortical regions because we only wanted to determine whether the cortical regions support visceromotor control. †Connection from dpIns/dmIns to sgACC not evident in several monkey studies[157,168,179–181] that have the potential to show it. ‡The medial portion of the vaIns exhibits connectivity with subcortical and brainstem regions, but not the lateral portion of the vaIns[43,182]. §Connection from sgACC to dpIns/dmIns and from pACC to dpIns/dmIns not evident in several monkey studies[146,167,179,180] that have the potential to show them, although weak, direct connectivity is evident in a recent tractography study in humans[183] (Fig. 5). Moreover, connections between sgACC, pACC and dpIns have been observed in intrinsic functional connectivity analyses in humans (for example, Fig. 6 of ref. [184]). The discrepancy between human findings and the tract-tracing studies in monkeys failing to show connectivity might reflect an expansion of Brodmann area (BA) 24 anterior and ventral to the corpus callosum in humans relative to monkeys and/or the presence of connections between BAs 25/32 and the posterior insula in humans that do not exist in monkeys (H. Evrard, personal communication). BA, Brodmann area.

from non-human tract-tracing studies: hypothalamus–dAmy, hypothalamus–dpIns, PAG–dAmy, PAG–medial ventral anterior insula (mvaIns) and NTS–subgenual anterior cingulate cortex (sgACC). This is approximately what we would expect by chance; however, there are several factors that might account for why these predicted connections did not materialize in our discovery and replication samples. First, all discrepancies involved the sgACC, PAG or hypothalamus, whose BOLD data exhibit poor signal-to-noise ratio because of their small size and their proximity to white matter or pulsating ventricles and arteries[57]. Second, individual differences in anatomical structure can make inter-subject alignment challenging, particularly in 3 T imaging of the brainstem where clear landmarks are not always available. Of the connections that did not replicate, one involved the anterior insula; there is some disagreement in the macaque anatomical literature as to the exact location of the anterior insula[45,58–60], which might help to explain any lack of correspondence between intrinsic and tract-tracing findings that we observed.

Validating the functions of the allostatic–interoceptive system in humans. The allostatic–interoceptive system reported in Fig. 3 was replicated in the validation sample (η^2 mean = 0.84, s.d. = 0.05 compared with discovery-sample cortical maps; η^2 mean = 0.76, s.d. = 0.07 compared with discovery-sample subcortical maps). These η^2 values are respectable and demonstrate adequate reliability of the system according to conventional psychometric theory, although the lower η^2 values are likely to be due to the smaller sample size, which magnifies the effects of poor signal-to-noise ratio in subcortical regions. Convergent validity for the proposed allostatic–interoceptive system was demonstrated, in that individuals with stronger functional connectivity within the system also reported greater arousal while viewing images that evoked greater activity in the sympathetic nervous system. Participants viewed 90 evocative photos known to induce a range of autonomic nervous system changes and corresponding feelings of arousal[61], as well as changes in BOLD activity within these regions[62,63]. We predicted, and found, that individuals showing stronger intrinsic connectivity within the

© 2017 Macmillan Publishers Limited, part of Springer Nature. All rights reserved.

allostatic–interoceptive system (specifically, connectivity between dpIns and anterior midcingulate cortex (aMCC)) also demonstrated a stronger concordance between objective and subjective measures of bodily arousal while viewing allostatically relevant images ($P = 0.003$; see Supplementary Fig. 8; see Supplementary Discussion for details).

There were three reasons for demonstrating the convergent validity of the proposed allostatic–interoceptive system using this task. First, there is a decades-old body of research indicating that interoception enables the subjective experience of arousal[64–66]. Thus, the amount of joint information shared by an objective, psychophysiological measure of visceromotor change (skin conductance) and the subjective experience of arousal (self-report ratings) is an implicit, behavioural measure of interoceptive ability. Indeed, individuals with more accurate interoceptive ability exhibit a stronger correspondence between subjective arousal and physiological arousal in response to similar evocative photos[67]. Second, explicit reports of interoceptive performance on heartbeat detection tasks[68–70] are complex to interpret neurally because they require synthesizing and comparing information from other systems (somatosensory system[71], frontoparietal control systems and, for heartbeat detection, the auditory system); in addition, these tasks are sometimes too hard (yielding floor effects) or have questionable validity[70].

At this juncture, it is tempting to ask whether the unified allostatic–interoceptive system is specific to allostasis and interoception. From our perspective, this is the wrong question to be asking. The past two decades of neuroscience research have brought us to the brink of a paradigm shift in understanding the workings of the brain, setting the stage to revolutionize brain:mind mapping. Neuroscience research is increasingly acknowledging that brain networks have a one (network) to many (function) mapping[28–30,72–74]. Our findings contribute to this discussion: a brain system that is fundamental to allostasis and interoception is not unique to those functions, but instead is also important for a wide range of psychological phenomena that span cognitive, emotional and perceptual domains (Fig. 5). This finding is not a failure of reverse inference; it suggests a functional feature of how the brain works.

Table 3 | Seeds used for intrinsic connectivity analyses

Seed	Type of region predicted by EPIC model	Cortical lamination	MNI coordinates
dpIns	Primary interoceptive cortex	Granular	36, −32, 16[185]
dmIns	Primary interoceptive cortex	Dysgranular	41, 2, 3[186]
sgACC	Visceromotor control	Agranular	2, 14, −6[187]
pACC	Visceromotor control	Agranular	13, 44, 0[185]
aMCC	Visceromotor control	Agranular	9, 22, 33[188]
mvaIns	Visceromotor control	Agranular	30, 16, −14[189]
lvaIns	Sensory integration	Agranular	44, 6, −15[188]
dAmy	Visceromotor control	N/A	27, 3, −12[190]

Note: all seeds are in the right hemisphere. Evidence for cortical lamination comes from ref. [42] (see also refs [191,192]).

Each anatomical region of interest was represented by one 4-mm-radius seed except for the vaIns, which required a medial and a lateral seed (mvaIns and lateral vaIns (lvaIns), respectively) to capture the previously established functional distinction between the medial visceromotor network (containing mvaIns) and the orbital sensory integration network (containing lvaIns) in the orbitofrontal cortex[182]. MNI, Montreal Neurological Institute.

Discussion

The integrated allostatic–interoceptive brain system is a complex cortical and subcortical system consisting of connected intrinsic networks. Our work demonstrates a single brain system that supports not just allostasis but also a wide range of psychological phenomena (emotions, memory, decision-making, pain) that can all be explained by their reliance on allostasis. Other studies have already shown that regions controlling physiology are also regions that control emotion. In fact, this was Papez's original logic for assuming that the 'limbic system' was functionally for emotion. This paper goes beyond this observation. Regions controlling inner body physiology lie in networks that also support social affiliation, pain, judgements, empathy, reward, addiction, memory, stress, craving and decision-making, among others (Fig. 5). More and more, functional imaging studies[30] are finding that the salience and default mode networks are domain-general (see previous reviews[28,29]). Our paper provides the groundwork for a theoretical and empirical framework for making sense of these findings in an anatomically principled way.

Our investigation was strengthened by our theoretical framework (the EPIC model[11]), the converging evidence from structural studies of the brain (tract-tracing studies in monkeys plus the well-validated structural model of information flow), our use of multiple methods (intrinsic connectivity in humans, as well as brain–behaviour relationships) and our ability to replicate the system in three separate samples totalling over 600 human participants. Our results are consistent with prior anatomical and functional studies that have investigated portions of this system at cortical and subcortical levels[17,18,26,27,75–78], including evidence that limbic cortical regions control the brainstem circuitry involved with allostatic functions such as cardiovascular control, respiratory control and thermoregulatory control[79], as well as prior investigations that focused on the intrinsic connectivity of individual regions such as the insula[80], the cingulate cortex[81], the amygdala[82] and the ventromedial prefrontal cortex[83]; but our results go beyond these prior studies in several ways. First, we observed an often-overlooked finding when interpreting the functional significance of certain brain regions: the dorsomedial prefrontal cortex, the ventrolateral prefrontal cortex, the hippocampus and several other regions have both a structural and functional pattern of connectivity that indicates their role in visceromotor control. A second often-overlooked finding is that relatively weaker connectivity patterns (for example between the visceromotor sgACC and the primary interoceptive cortex) are reliable, and future studies may find that they are of functional significance. Third, we demonstrated behavioural relevance of connectivity within this network, something that prior studies of large-scale autonomic control networks have yet to test[75–77].

Taken together, our results strongly support the EPIC model's hypothesis that visceromotor control and interoceptive inputs are integrated within one unified system[11], as opposed to the traditional view that the cerebral cortical regions sending visceromotor signals and those that receive interoceptive signals are organized as two segregated systems, similar to the corticospinal skeletomotor efferent system and the primary somatosensory afferent system.

Perhaps most importantly, the allostatic–interoceptive system has been shown to have a role in a wide range of psychological phenomena, suggesting that allostasis and interoception are fundamental features of the nervous system. Anatomical, physiological and signal processing evidence suggests that a brain did not evolve for rationality, happiness or accurate perception; rather, all brains accomplish the same core task[20]: to efficiently ensure resources for physiological systems within an animal's body (its internal milieu) so that an animal can grow, survive, thrive and reproduce. That is, the brain evolved to regulate allostasis[21]. All psychological functions performed in the service of growing, surviving, thriving and reproducing (such as remembering, emoting, paying attention or deciding) require the efficient regulation of metabolic and other biological resources.

Our findings add an important dimension to the existing observations that the default mode and salience networks serve as a high-capacity backbone for integrating information across the entire brain[84]. Diffusion tensor imaging studies indicate, for example, that these two networks contain the highest proportion of hubs

© 2017 Macmillan Publishers Limited, part of Springer Nature. All rights reserved.

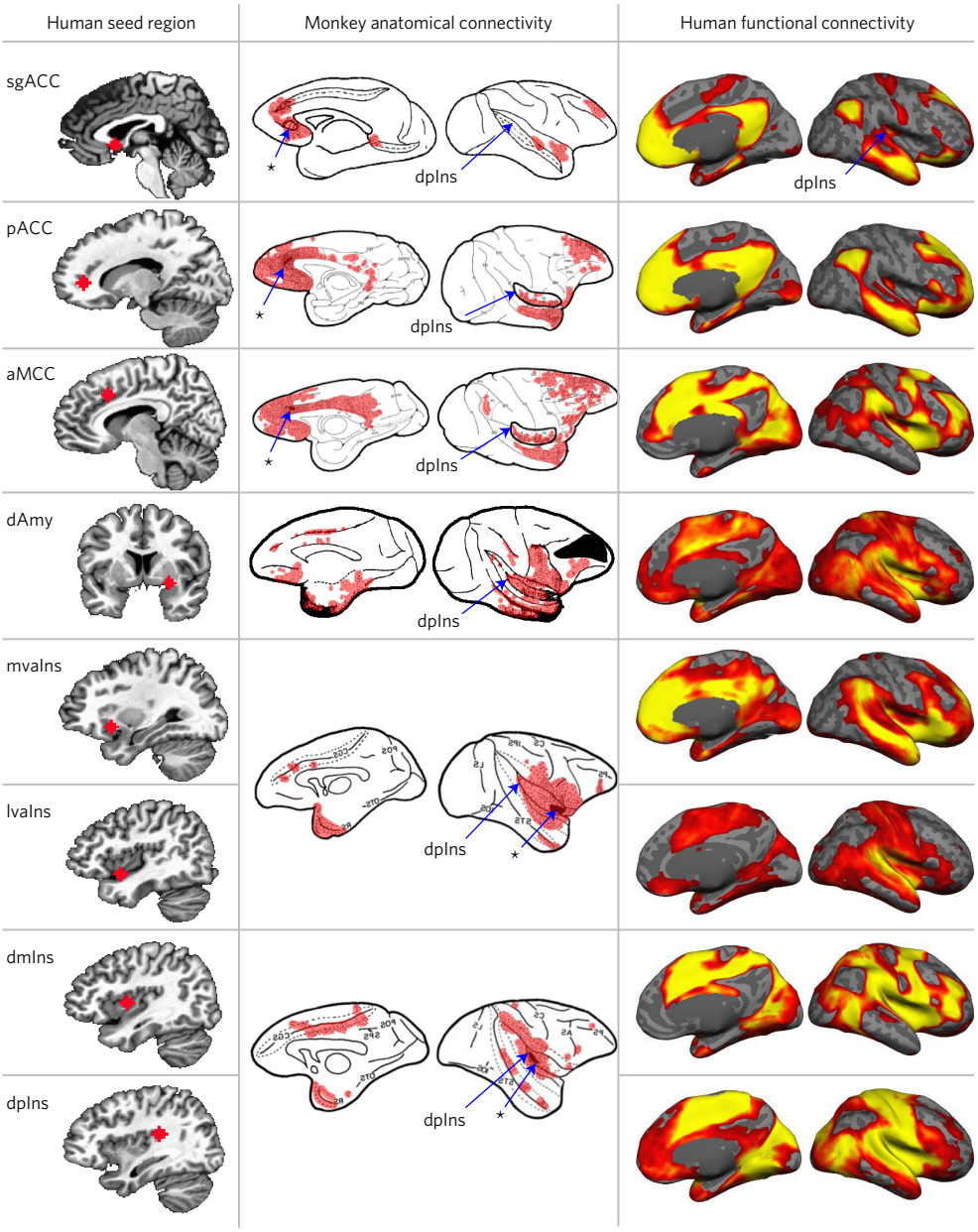

Figure 2 | Eight regions ('seeds') used to estimate the unified allostasis/interoceptive system connecting the cortical and amygdalar visceromotor regions and primary interoceptive regions. The left column shows the seed region for each discovery map on a human brain template. The middle column summarizes the anatomical connectivity derived from anterograde and/or retrograde tracers injected into macaque brains at a location homologous to the human seed (asterisks with blue arrows). The right column shows the human intrinsic connectivity discovery maps depicting all voxels whose time course is correlated with that of the seed (ranging from $P < 10^{-5}$ in red to $P < 10^{-40}$ in yellow, uncorrected, $N = 280$). To avoid type I and type II errors, which are enhanced with the use of stringent statistical thresholds[195], we opted to separate signal from random noise using replication, according to the mathematics of classical measurement theory[147]. These results were replicated in a second sample, $N = 270$ participants, indicating that they are reliable and cannot be attributed to random error (Supplementary Fig. 1). Functional connectivity to the entire amygdala and other subcortical regions are shown in Fig. 4. The monkey anatomical connectivity figures were coloured red to visualize results, and some were mirrored to match the orientation of the human brain maps. Tract-tracing figures (middle column) adapted with permission from: sgACC, ref. [168], John Wiley and Sons; pACC and aMCC, ref. [156], Elsevier; dAmy, ref. [164], Elsevier; mvaIns, lateral vaIns (lvaIns), dmIns and dpIns, ref. [157], John Wiley and Sons. The figures from ref. [156] were adapted to show the insula in its lateral view.

belonging to the brain's 'rich club', defined as the most densely interconnected regions in the cortex[73,85] (several of which are connector hubs within the allostatic–interoceptive system; see Fig. 3 and Supplementary Table 4). All other sensory and motor networks communicate with the default mode and salience networks, and potentially with one another, through these hubs[1,85]. The agranular hubs within the two networks, which are also visceromotor control regions, are the most powerful predictors in the brain[11,32]. Indeed, hub regions in these networks display a pattern of connectivity that positions them to easily send prediction signals to every other sensory system in the brain[12,32].

The fact that default mode and salience networks are concurrently regulating and representing the internal milieu, while they are routinely engaged in a wide range of tasks spanning cognitive,

© 2017 Macmillan Publishers Limited, part of Springer Nature. All rights reserved.

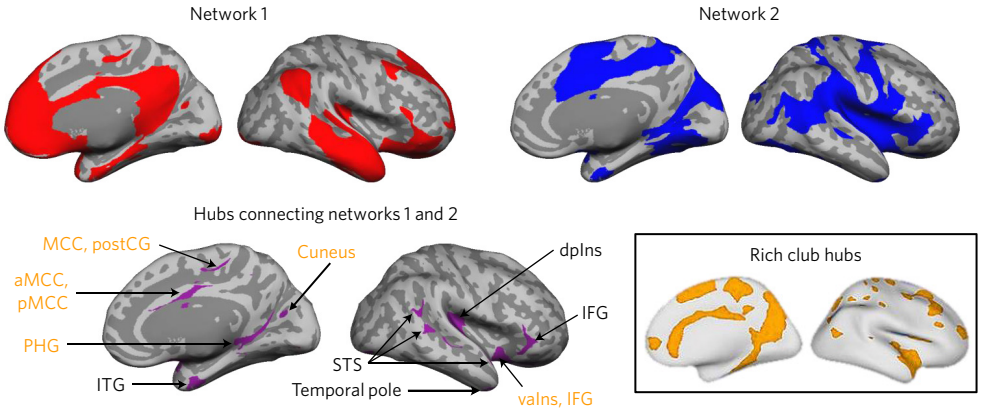

Figure 3 | The unified allostatic–interoceptive system is composed of two large-scale intrinsic networks that share several hubs. Networks of the unified allostatic–interoceptive system are shown in red and blue, and hubs are shown in purple; for coordinates, see Supplementary Table 4. Hubs belonging to the 'rich club' are shown in yellow. Rich club hubs figure adapted with permission from ref. [85], Society for Neuroscience. All maps result from the sample of 280 participants binarized at $P < 10^{-5}$ uncorrected from a one-sample two-tailed *t*-test. These results were replicated in a second sample, $N = 270$ participants, indicating that they are reliable and cannot be attributed to random error (Supplementary Fig. 2). IFG, inferior frontal gyrus; ITG, inferior temporal gyrus; PHG, parahippocampal gyrus; pMCC, posterior midcingulate cortex; postCG, postcentral gyrus; STS, superior temporal sulcus.

perceptual and emotion domains, all of which involve value-based decision-making and action[30,86–90], suggests a provocative hypothesis for future research: whatever other psychological functions the default mode and salience networks are performing during any given brain state, they are simultaneously maintaining or attempting to restore allostasis and are integrating sensory representations of the internal milieu with the rest of the brain. Therefore, our results, when situated in the published literature, suggest that the default mode and salience networks create a highly connected functional ensemble for integrating information across the brain, with interoceptive and allostatic information at its core, even though it may not be apparent much of the time.

When understood in this framework, our current findings do more than just add more functions to the ever-growing list attributed to the default mode and salience networks (which currently spans cognition, attention, emotion, perception, stress and action[28,30]). Our results offer an anatomically plausible computational hypothesis for a set of brain networks that have long been observed but the functions of which have not been fully understood. The observation that allostasis (regulating the internal milieu) and interoception (representing the internal milieu) are at the anatomical and functional core of the nervous system[18,20] offers a generative avenue for further behavioural hypotheses. For example, it has recently been observed that many of the visceromotor regions within the unified allostatic–interoceptive system contribute to the ability of 'SuperAgers' to perform memory and executive function tasks like much younger people[91].

Furthermore, our findings also help to shed light on two psychological concepts that are constantly confused in the psychological and neuroscience literatures: affect and emotion. If, whatever else your brain is doing — thinking, feeling, perceiving, moving — it is also regulating your autonomic nervous system, your immune system and your endocrine system, then it is also continually representing the interoceptive consequences of those physical changes. Interoceptive sensations are usually experienced as lower-dimensional feelings of affect[23,92]. As such, the properties of affect — valence and arousal[93,94] — can be thought of as basic features of consciousness[95–101] that, importantly, are not unique to instances of emotion.

Perhaps the most valuable aspect of our findings is in moving beyond traditional domain-specific or 'modular' views of brain structure/function relationships[102], which assume a significant degree of specificity in the functions of various brain systems. A growing body of evidence requires that these traditional modular views be abandoned[28,103,104] in favour of models that acknowledge that neural populations are domain-general or multi-use. The idea of domain-generality even applies to primary sensory networks, as evidenced by the fact that multisensory processing occurs in brain regions that are traditionally considered unimodal (for example, the auditory cortex responding to visual stimulation[105,106]). The absence of specificity in brain structure/function relationships is not a measurement error or some biological dysfunction, but a useful feature that reflects core principles of biological degeneracy that are also evident in the genome, the immune system and every other biological system shaped by natural selection[107].

No study is without limitations. First, there are potential issues in identifying homologous regions between monkey and human brains[47]; nonetheless, we still found evidence for most of the monosynaptic connections predicted by the EPIC model. Second, we used

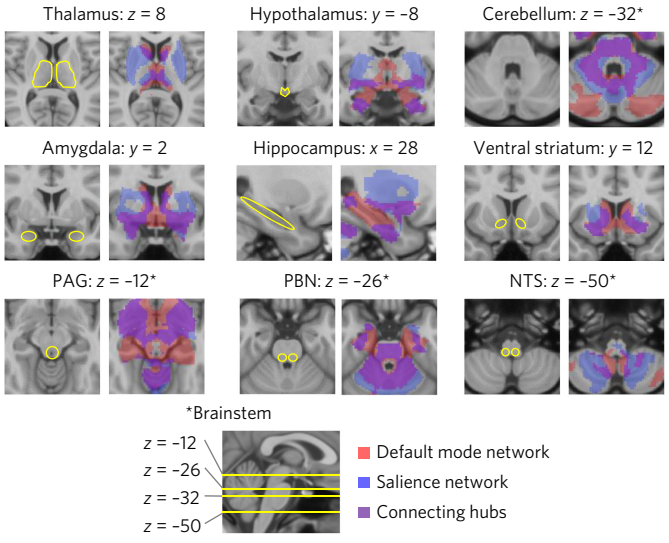

Figure 4 | Subcortical connectivity of the two integrated intrinsic networks within the allostatic–interoceptive system ($N = 280$; $P < 0.05$ uncorrected). These results were replicated in a second sample of $N = 270$ (Supplementary Fig. 5). *x*, *y* and *z* refer to the MNI coordinates in mm.

© 2017 Macmillan Publishers Limited, part of Springer Nature. All rights reserved.

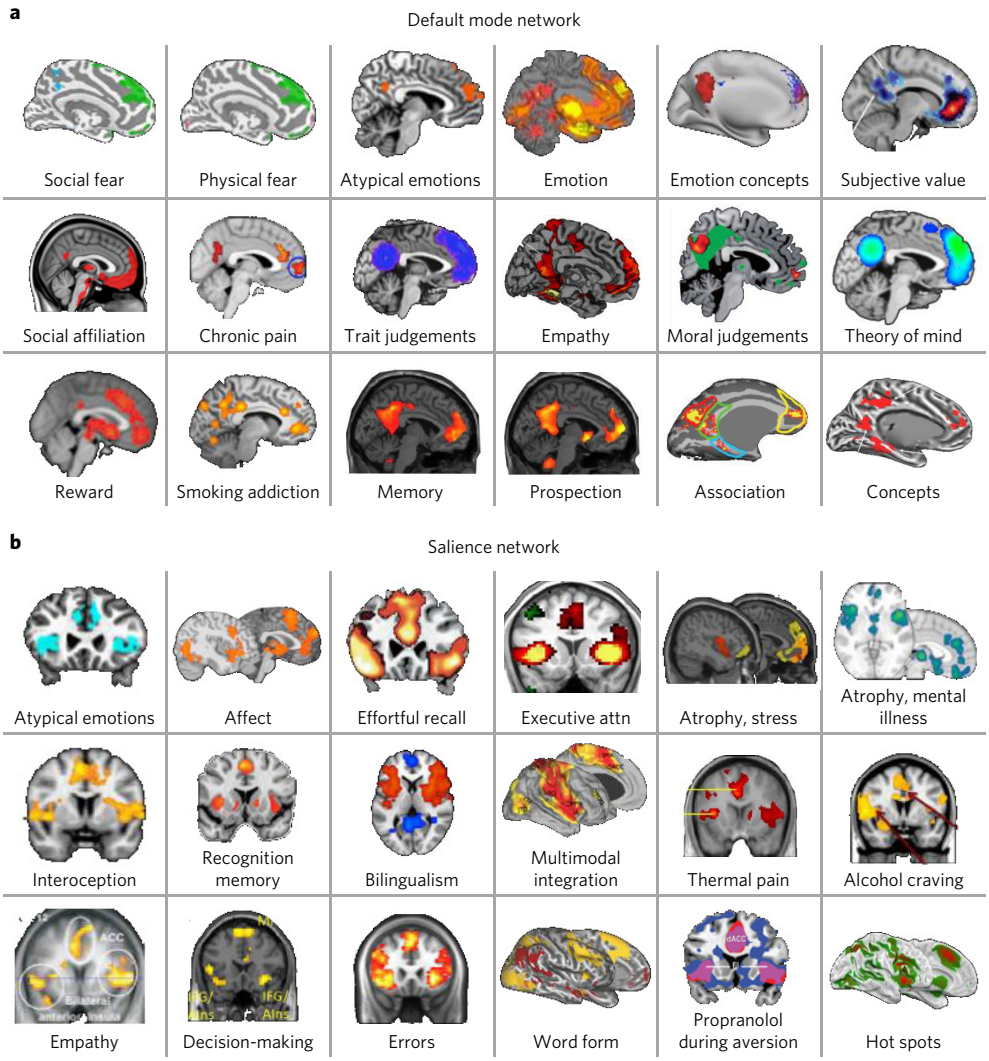

Figure 5 | The default mode and salience networks each support a wide array of psychological functions. Evidence for this comes from a literature review of psychological or other states that are sensitive to functional or structural features of these networks. These results are consistent with the idea that the default mode (**a**) and salience (**b**) networks are domain-general networks that support interoception and allostasis, which we propose are key processes that contribute to all psychological functions. Each sub-figure shows a set of results from an independent study, reproduced with permission from: **a**, atypical emotions, ref. [197], Oxford Univ. Press; emotion, ref. [198], Elsevier; emotion concepts, ref. [199], Elsevier; subjective value, ref. [200], Oxford Univ. Press; social affiliation, ref. [201], Society for Neuroscience; chronic pain, ref. [202], PLOS; trait judgements and theory of mind, ref. [203], Elsevier; empathy, ref. [204], Frontiers; moral judgements, ref. [205], Oxford Univ. Press; reward, ref. [206], Elsevier; smoking addiction, ref. [207], Elsevier; memory and prospection, ref. [208], The Royal Society; association, ref. [209], Wiley; concepts, ref. [210], Oxford Univ. Press; **b**, atypical emotions, ref. [197], Oxford Univ. Press; affect, ref. [211], Oxford Univ. Press; effortful recall, ref. [212], Wiley; executive attention, ref. [213], © 2007 National Academy of Sciences; atrophy and stress (chronic, yellow; current, red), ref. [214], Elsevier; atrophy and mental illness, ref. [122], American Medical Association; interoception, ref. [215], Wiley; recognition memory, ref. [216], Frontiers; bilingualism, ref. [217], Elsevier; multimodal integration, ref. [1], Society for Neuroscience; thermal pain, ref. [218], Elsevier; alcohol craving, ref. [219], Wiley; empathy, ref. [220], AAAS; decision-making, ref. [221], Frontiers; errors, ref. [222], Society for Neuroscience; word form (yellow), ref. [223], Society for Neuroscience; propranolol during aversion, ref. [224], AAAS; hot spots, ref. [225], Guildford Press. Data used to make the sub-figures showing social and physical fear (**a**) taken from ref. [196].

an indirect measure of brain connectivity in humans (functional connectivity analyses of low-frequency BOLD data acquired at rest) that reflects both direct and indirect connections and can, in principle, inflate the extent of an intrinsic network[47]. Moreover, low-frequency BOLD correlations may reflect vascular rather than neural effects in the brain[108]. Nonetheless, our results exhibit specificity: the integrated allostatic–interoceptive system conforms to well-established salience and default mode networks and is remarkably consistent with both cortical and subcortical connections repeatedly observed in tract-tracing studies of non-human animals. Third, although our fMRI procedures were not optimized to identify subcortical and brainstem structures and study their connectivity (for examples of optimization, see refs [57,75,76,109]), we nonetheless observed 92% of the predicted connectivity results. Finally, many studies find that activities in the default mode and salience networks have an inverse or negative relationship (sometimes referred to as 'anti-correlated'), meaning that as one network increases its neural activity relative to baseline, the other decreases. Such findings and interpretations have recently been challenged on both statistical and theoretical grounds[110] (see Supplementary Discussion). In fact, when global signal is not removed in pre-processing, the two networks can show a pattern of positive connectivity[111]. Fourth, our demonstration of a brain/behaviour relationship (using the evocative pictures) was merely a preliminary evaluation of how individual differences in the function of this system are related to individual differences in behaviour. Additionally, our use of electrodermal activity as a

© 2017 Macmillan Publishers Limited, part of Springer Nature. All rights reserved.

measure of sympathetic nervous system activity is arguably too specific because different components of the sympathetic nervous system react differently[112], and peripheral sensations associated with changes in electrodermal activity might not be processed by the interoceptive brain circuitry that we are studying here, thus complicating the interpretation of our results. However, we did not intend to assess a specific neural pathway carrying information about electrodermal activity, and we believe that — despite their limitations — our results are useful and hypothesis-generating. Future work is needed for a more thorough understanding of this and other brain–behaviour relationships involving this system.

This project is one in a series of studies to precisely test the EPIC model, including its predictive coding features (not just the anatomical and functional correlates as shown here). Future research must focus on the ongoing dynamics by which the default mode and salience networks support allostasis and interoception, including the predictions that they issue to other sensory and motor systems. It is possible, for example, that both networks use past experience in a generative way to issue prediction signals, but that the default mode network generates an internal model of the world via multisensory predictions (consistent with previous work[113–115]), whereas the salience network issues predictions, as precision signals, to tune this model with prediction error (consistent with the salience network's role in attention regulation and executive control; for example refs[51,116,117]). Unexpected sensory inputs that are anticipated to have allostatic implications (that is, likely to impact survival, offering reward or threat) will be encoded as 'signal' and learned, so as to support allostasis better in the future, with all other prediction error treated as 'noise' and safely ignored[118] (for discussion, see ref. [119]). These and other hypotheses regarding the flow of predictions and prediction errors in the brain (for example incorporating the cerebellum, ventral striatum and thalamus[24]) can be tested using new methods such laminar MRI scanning at high (7 T) magnetic field strengths[120].

Future research that provides a more mechanistic understanding of how the default mode and salience networks support interoception and allostasis will also reveal insights into the mind–body connections at the root of mental and physical illness and their comorbidities. For example, in illness, the neural representations of the world that underlie action and experience may be directed more by predicted allostatic relevance of information than by the need for accuracy and completeness in representing the environment. Indeed, atrophy and dysfunction within parts of the interoceptive system are considered common neurobiological substrates for mental and physical illness[121–123], including depression[124], anxiety[125], addiction[126], chronic pain[127], obesity[128] and chronic stress[129,130]. By contrast, increased cortical thickness in the MCC is linked to the preserved memory of 'SuperAgers' relative to their more typically performing elderly peers[131,132], suggesting a potential mechanism for how exercise (via the sustained visceromotor regulation it requires) benefits cognitive function in aging[133] and why certain activities, such as mindfulness or contemplative practice, can be beneficial[134,135]. Ultimately, a better understanding of how the mind is linked to the physical state of the body through allostasis and interoception may help to resolve some of the most critical health problems of our time, such as the comorbidities among mental and physical disorders related to metabolic syndrome (for example depression and heart disease[136]) or how chronic stress speeds cancer progression[137], as well as offering key insights into the emergence of public health issues related to addiction and mental illness, such as opioid use[138] and suicides[139].

Methods

Participants. *Discovery and replication samples.* We randomly selected 660 participants (365 female, 55%, 18–30 years) from 1,000 healthy participants described in previous work[55,140]. The 1,000 participants were native English-speaking adults, 18–35 years, with normal or corrected-to-normal vision, and reported no history of neurological or psychiatric conditions. We removed 79 participants (11%) owing to head motion and outlying voxel intensities; we removed 31 more participants (4.7%) owing to lack of signal in superior and lateral parts of the brain (see section on analysis of fMRI data). Our final dataset of 550 participants was randomly divided into a discovery sample of $N = 280$ (174 female, 62%, mean = 19.3 years, s.d. = 1.4 years) and a replication sample of $N = 270$ (142 female, 53%, mean = 22.3 years, s.d. = 2.1 years).

We also randomly selected 150 participants (75 female, 50%, mean = 22.5, s.d. = 2.0 years) from the $N = 1,000$ in order to generate maps of the established default mode and salience networks.

Validity sample. We selected all 66 young and middle-aged participants (33 female, 18–60 years, mean = 34.8 years, s.d. = 13.8 years) from an existing dataset of 111 participants (56 female, 18–81 years, mean = 46.6 years, s.d. = 18.9 years) recruited from the Boston area during 2012–2014 for a study examining age-related changes in how affect supports memory[141]. Only 41 participants (14 female, 47%, 20–60 years, mean = 33.8 years, s.d. = 14.1 years) had both high-quality fMRI BOLD data and sufficient electrodermal activity changes according to previously established procedures (see Analysis sections). Specifically, 12 participants exhibited excessive head motion and outlying voxel intensities, and 16 participants lacked electrodermal responses. Participants were right-handed, native English speakers and had normal or corrected-to-normal vision. None reported any history of neurological or psychiatric condition, learning disability or serious head trauma. Participants did not smoke and did not ingest substances (such as beta-blockers or anti-cholinergic medications) that interfere with autonomic responsiveness.

Sample size. No pre-specified effect size was known, so we used a large portion of a third-party dataset ($N = 660$) and the maximum size of a second dataset collected in our laboratory with young and middle-aged adults ($N = 66$).

Procedure. *Discovery and replication samples.* Participants provided written informed consent in accordance with the guidelines set by the institutional review boards of Harvard University or Partners Healthcare. Participants completed MRI structural and resting-state scans and other tasks unrelated to the current analysis. MRI data were acquired at Harvard and the Massachusetts General Hospital across a series of matched 3 T Tim Trio scanners (Siemens, Erlangen, Germany) using a 12-channel phased-array head coil. Structural data included a high-resolution multi-echo T1-weighted magnetization-prepared gradient-echo image (multi-echo MP-RAGE). Parameters for the structural scan were as follows: repetition time (TR) = 2,200 ms, inversion time (TI) = 1,100 ms, echo time (TE) = 1.54 ms for image 1 to 7.01 ms for image 4, flip angle (FA) = 7°, voxel size 1.2 × 1.2 × 1.2 mm and field of view (FOV) = 230 mm. The functional resting state scan lasted 6.2 min (124 time points). The echo planar imaging (EPI) parameters for functional connectivity analyses were as follows: TR = 3,000 ms, TE = 30 ms, FA = 85°, voxel size 3 × 3 × 3 mm, FOV = 216 mm and 47 axial slices collected with interleaved acquisition and no gap between slices.

Validity sample. Participants provided consent in accordance with the institutional review board. Data were acquired on separate sessions across several days. The first session consisted of a 6-min seated baseline assessment of peripheral physiology, the EXAMINER cognitive battery[142], a second 6-min seated baseline, the evocative images task and other tasks. Only the evocative images task is relevant for this study. Electrodes were placed on the chest, hands and face to record electrocardiogram, electrodermal activity and facial electromyography, respectively. A belt with a piezoelectric sensor was secured on the chest to record respiration. Only the electrodermal activity data are reported here. Electrodermal activity was recorded using disposable electrodermal electrodes (containing isotonic paste) affixed to the thenar and hypothenar eminences of the left hand. Data were collected using BioLab v3.0.13 (Mindware Technologies, Gahanna, OH, USA). Participants sat upright in a comfortable chair in a dimly lit room. Ninety full-colour photos were selected from the International Affective Picture System (IAPS) and used to induce affective experiences[61]. The pictures were selected based on normative ratings of pleasure/displeasure (valence) and arousal experienced when viewing them (unpleasant–high arousal, pleasant–high arousal, unpleasant–low arousal, pleasant–low arousal, neutral valence–low arousal; Supplementary Table 5). Participants viewed the photos sequentially on a 120 × 75-cm high-definition screen 2 metres away. Photos were grouped into three blocks of 30 each, with the order of the photos within each block fully randomized. For each trial, participants viewed an IAPS photo for 6 seconds, and then rated their experience for valence and arousal using the self-assessment manikin (SAM[143]). Only the arousal ratings are relevant to this report, and they ranged from 1 ('very calm') to 5 ('very activated'). A variable inter-trial interval of 10–15 seconds followed the rating prior to presentation of the next picture. Before beginning the task, participants were familiarized with the SAM rating procedure and practised by rating five pictures. The photos and rating scales were administered via E-Prime (Psychology Software Tools, Pittsburgh, PA).

The second laboratory testing session involved MRI scanning, consisting of a structural scan, resting state scan and other tasks unrelated to the present report (presented elsewhere[141]). MRI data were acquired using a 3 T Tim Trio scanner (Siemens, Erlangen, Germany) with a 12-channel phased-array head coil. Structural data included a high-resolution T1-weighted MP-RAGE with TR = 2,530 ms,

© 2017 Macmillan Publishers Limited, part of Springer Nature. All rights reserved.

TE = 3.48 ms, FA = 7° and 1×1×1-mm isotropic voxels. The functional resting-state scan lasted 6.40 min (76 time points). The EPI parameters were as follows: TR = 5,000 ms, TE = 30 ms, FA = 90°, 2×2×2-mm voxels and 55 axial slices collected with interleaved acquisition and no gap between slices. Participants were instructed to keep their eyes open without fixating and remain as still as possible.

Selection of regions in the interoceptive/allostatic system. We selected several cortical regions with established visceromotor connections, including regions in the insula and ACC (Table 1). We also included the dAmy in our system because its central nucleus is known to have key visceromotor functions (for a review, see ref. [144]); the dAmy, being a subcortical region, does not have a laminar structure, but there are connections between the amygdala and primary interoceptive cortex (dmIns/dpIns[60,145,146]) that are predicted by the EPIC model (using Barbas's structural model of information flow within the cortex). Similarly, the anterior cingulate cortex (ACC), a key limbic visceromotor region, is connected with the amygdala in a pattern consistent with the EPIC model hypothesis that the ACC sends visceromotor prediction signals to the central nucleus (the ACC primarily sends output from its deep layers and receives input from the amygdala in its upper layers[147]). Currently, there are insufficient data to test the EPIC model hypothesis that amygdala projections terminate in the upper layers of dmIns/dpIns and that the amygdala receives inputs from its deep layers, as these data are not available in prior tract-tracing studies involving the insula and amygdala[60,145,146].

Analysis of task-independent ('resting-state') fMRI data. *Quality assessment.* We applied established censoring protocols for head motion and outlying signal intensities using AFNI (https://afni.nimh.nih.gov/afni/) following ref. [148] and described in the following three steps. First, we disqualified an fMRI volume if AFNI's 'enorm motion' derivative parameter (derived from afni_proc.py) was greater than 0.3 mm. Second, we disqualified an fMRI volume if the fraction of voxels with outlying signal intensity (AFNI's 3dToutcount command) was greater than 0.05. Third, if a volume surpassed either criterion, we removed that volume, the prior volume and the next two volumes. In a separate procedure, we disqualified discovery and replication participants who lost more than 10% of their 124 volumes owing to either criterion (79 participants, 11%). Quality assessment for surface-based processing required removing 31 additional participants (4.7%) owing to a lack of signal in the most superior and lateral parts of the brain, which would result in incomplete group connectivity maps; no participants were removed for this reason in the validity sample. In the validity sample, we removed participants who lost more than 40% of their 76 volumes, removing 12 participants (18%); we used a more lenient threshold because of the small sample size ($N = 66$). The fraction of volumes censored per participant using the aforementioned approach[140] yielded nearly identical results to another established censoring approach[149] as implemented in AFNI's afni_restproc.py script.

Preprocessing. We applied standard Freesurfer preprocessing steps to both samples of resting-state data (http://surfer.nmr.mgh.harvard.edu). These included removal of the first four volumes, motion correction, slice timing correction, resampling to the MNI152 cortical surface (left and right hemispheres) and MNI305 subcortical volume (2-mm isotropic voxels), spatial smoothing (6 mm full-width at half-maximum (FWHM), surface and volume separately) and temporal filtering (0.01-Hz high-pass filter and 0.08-Hz low-pass filter). We did not use global signal regression in order to prevent spurious negative correlations ('anti-correlated networks'), which can interfere with interpreting the connectivity results[110].

Functional connectivity analysis. We estimated cortical connectivity using surface-based analyses, affording more sensitive and reliable discovery maps and reducing artifacts around sulcal and opercular borders by registering each participant's native space to MNI152 space via Freesurfer's reconstruction of each participant's cortical surfaces[150]. The surface-based intrinsic analyses also allowed us to incorporate the selected subcortical seed (dAmy), but did not allow us to analyse connectivity to subcortical structures more broadly. We first created a 4-mm-radius sphere centred on the MNI coordinates identified in Table 3 and found the vertex on the MNI152 pial surface that is closest to the spherical seed. We then smoothed this single vertex by 4 mm on the surface and mapped the resulting cortical label to each individual subject's cortex. The individual cortical label was projected back into the subject's native volumetric space to calculate the averaged time series within the seed. For the subcortical seed (dAmy), we directly projected the spherical seed into each subject's native volumetric space and extracted its time course. On the subject level, we ran a voxel-wise regression on left and right hemispheres of MNI152 and subcortical volume of MNI305 to compute the partial correlation coefficient and correlation effect size of the seed time series, taking into account several nuisance variables: cerebrospinal fluid signal, white matter signal, motion correction parameters and a fifth-order polynomial. On the group level, we concatenated the contrast effect size maps from all subjects and ran a general linear model analysis to test whether the group mean differed from zero. This yielded final group maps that showed regions whose fluctuations significantly correlated with the seed's BOLD time series.

To estimate cortical–subcortical connectivity, we used a more liberal statistical threshold compared with the analyses of corticocortical connectivity. The smaller size of subcortical regions, as well as their anatomical placement, renders their signal noisier and less reliable[57], yielding relatively smaller estimates of intrinsic connectivity. Thus, guided by classical measurement theory[151], we relied on replication to determine which connectivity values were meaningful.

k-means cluster analysis of discovery maps. First, we computed the 8×8 η^2 similarity matrix for each pair of maps[49]. Based on visual inspection of the eight maps, we used *k*-means clustering with $k = 2$ and $k = 3$ using the kmeans function in MATLAB (Mathworks, Natick, MA). Our results confirmed that $k = 2$ captured the default mode versus salience distinction across these maps, whereas $k = 3$ further divided the 'salience cluster' into two sub-categories depending on whether somatosensory cortices are included. Because sub-categories within the salience network were not important to our study goals, we used the $k = 2$ cluster solution.

Identification of the interoceptive system networks. We confirmed that Network 1 is the established default mode network (for a review, see ref. [50]) and Network 2 is the established salience network[51,52]. The reference maps were constructed using coordinates obtained from previous work[55] as follows. Using a random sample of $N = 150$, we created a mask of the default mode network by conjoining functional connectivity maps from two hubs in the default mode network[55]: a 4-mm seed at the dorsomedial prefrontal cortex (MNI 0, 50, 24) and a 4-mm seed at the posterior cingulate cortex (MNI 0, −64, 40). We likewise created a mask of the salience network by conjoining functional connectivity maps from two bilateral hubs in the salience network (labelled as the ventral attention network in ref. [55]): 4-mm seeds at the left and right supramarginal gyrus (MNI ±60, −30, 28) and 4-mm seeds at the left and right anterior insula (MNI ±40, 12, −4). We thresholded our maps to $P < 10^{-5}$ uncorrected (as in all our analyses) and we thresholded the default mode and salience networks to $z(r) > 0.05$ where z is the Fisher's r-to-z transformation. We then calculated the percentage of each established network (default mode or salience) that covered each of our networks (Network 1 or 2), and the complementary measure: the percentage of each of our networks (Network 1 or 2) that covered each established network (default mode or salience). These calculations used only the right hemisphere.

Reliability analyses. We used η^2 as an index of reliability because it shows similarity between maps while discounting scaling and offset effects[49]. An η^2 value of 1 indicates spatially identical maps, while an η^2 value of 0.5 indicates statistically independent maps. For each of our eight cortical and amygdalar seeds, we calculated η^2 between the discovery and replication samples using the effect size (gamma) maps generated by the group-level general linear model analysis. Then we calculated the mean and s.d. of the eight η^2 values across all seeds to index overall similarity between samples. This was done separately for the cortical and subcortical maps. We repeated the same procedure to compare the reliability between the discovery and validation samples.

Analysis of the evocative images task. We analysed electrodermal activity data using Electrodermal Activity Analysis v3.0.21 (Mindware). For each 6-second trial when the photo was visible, we measured the number of event-related skin conductance responses (SCRs) according to best practices[152]. We considered a SCR to be event-related if both the response onset and peak occurred between 1 and 6 seconds after stimulus onset, with an amplitude ≥0.01 μS. It is commonly observed that a substantial proportion of healthy adults produce relatively few if any SCRs[153]. We disqualified 16 of our 66 participants (24%) because they generated event-related SCRs during fewer than 5% of the evocative photo trials. We analysed our data using the number of SCRs (as opposed to the amplitude of the SCRs) per prior work from our group (for example ref. [154]) and others (for example ref. [155]).

Multilevel linear modelling to assess correspondence between objective physiological and subjective arousal during an allostatically relevant task. We used HLM v7.01 with robust parameter estimates (Scientific Software International; Skokie, IL). Level-1 of the model estimated the linear relationship (slope and intercept) between physiological arousal (number of event-related SCRs) and subjective arousal (1 = 'very calm' to 5 = 'very activated') in response to each of 90 photos. Thus, the model was adjusted for mean individual reactivity. Level-2 estimated the extent to which intrinsic connectivity between viscerosensory and visceromotor regions (for example dpIns–aMCC) moderated the relationship between objective and subjective arousal (that is, moderated the slope of the Level 1 model). All variables were unstandardized. Level-1 variables were group-mean centred (for each participant) and Level-2 variables were grand-mean centred (across participants).

Data availability. The data that support the findings of this study are available from the corresponding authors upon request.

Code availability. The code to analyse data is available from the corresponding authors upon request.

Received 27 May 2016; accepted 13 February 2017; published 24 April 2017

© 2017 Macmillan Publishers Limited, part of Springer Nature. All rights reserved.

References

1. Sepulcre, J., Sabuncu, M. R., Yeo, T. B., Liu, H. & Johnson, K. A. Stepwise connectivity of the modal cortex reveals the multimodal organization of the human brain. *J. Neurosci.* **32,** 10649–10661 (2012).
2. Rao, R. P. & Ballard, D. H. Predictive coding in the visual cortex: a functional interpretation of some extra-classical receptive-field effects. *Nat. Neurosci.* **2,** 79–87 (1999).
3. Chennu, S. *et al.* Expectation and attention in hierarchical auditory prediction. *J. Neurosci.* **33,** 11194–11205 (2013).
4. Shipp, S. The importance of being agranular: a comparative account of visual and motor cortex. *Phil. Trans. R. Soc. Lond. B* **360,** 797–814 (2005).
5. Zelano, C., Mohanty, A. & Gottfried, J. A. Olfactory predictive codes and stimulus templates in piriform cortex. *Neuron* **72,** 178–187 (2011).
6. Kusumoto-Yoshida, I., Liu, H., Chen, B. T., Fontanini, A. & Bonci, A. Central role for the insular cortex in mediating conditioned responses to anticipatory cues. *Proc. Natl Acad. Sci. USA* **112,** 1190–1195 (2015).
7. Adams, R. A., Shipp, S. & Friston, K. J. Predictions not commands: active inference in the motor system. *Brain Struct. Funct.* **218,** 611–643 (2013).
8. Clark, A. Whatever next? Predictive brains, situated agents, and the future of cognitive science. *Behav. Brain Sci.* **36,** 181–204 (2013).
9. Friston, K. The free-energy principle: a unified brain theory? *Nat. Rev. Neurosci.* **11,** 127–138 (2010).
10. Pezzulo, G., Rigoli, F. & Friston, K. Active inference, homeostatic regulation and adaptive behavioural control. *Prog. Neurobiol.* **134,** 17–35 (2015).
11. Barrett, L. F. & Simmons, W. K. Interoceptive predictions in the brain. *Nat. Rev. Neurosci.* **16,** 419–429 (2015).
12. Chanes, L. & Barrett, L. F. Redefining the role of limbic areas in cortical processing. *Trends Cogn. Sci.* **20,** 96–106 (2016).
13. Seth, A. K. Interoceptive inference, emotion, and the embodied self. *Trends Cogn. Sci.* **17,** 565–573 (2013).
14. Seth, A. K., Suzuki, K. & Critchley, H. D. An interoceptive predictive coding model of conscious presence. *Front. Psychol.* **2,** 395–410 (2012).
15. Gu, X. & FitzGerald, T. H. Interoceptive inference: homeostasis and decision-making. *Trends Cogn. Sci.* **18,** 269–270 (2014).
16. Allen, M. & Friston, K. J. From cognitivism to autopoiesis: towards a computational framework for the embodied mind. *Synthese* http://dx.doi.org/10.1007/s11229-016-1288-5 (2016).
17. Craig, A. D. How do you feel? Interoception: the sense of the physiological condition of the body. *Nat. Rev. Neurosci.* **3,** 655–666 (2002).
18. Craig, B. *How Do You Feel? An Interoceptive Moment with Your Neurobiological Self* (Princeton Univ. Press, 2014).
19. Sherrington, C. in *Textbook of Physiology* (ed. Schäfer, E. A.) 920–1001 (Pentland, 1900).
20. Sterling, P. & Laughlin, S. *Principles of Neural Design* (MIT Press, 2015).
21. Sterling, P. Allostasis: a model of predictive regulation. *Physiol. Behav.* **106,** 5–15 (2012).
22. McEwen, B. S. & Stellar, E. Stress and the individual. Mechanisms leading to disease. *Arch. Intern. Med.* **153,** 2093–2101 (1993).
23. Barrett, L. F. *How Emotions Are Made: The Secret Life of the Brain* (Houghton Mifflin Harcourt, 2017).
24. Barrett, L. F. The theory of constructed emotion: an active inference account of interoception and categorization. *Soc. Cogn. Affect. Neurosci.* http://dx.doi.org/10.1093/scan/nsw154 (2016).
25. Barrett, L. F., Quigley, K. S. & Hamilton, P. An active inference theory of allostasis and interoception in depression. *Phil. Trans. R. Soc. B* **371,** http://dx.doi.org/10.1098/rstb.2016.0011 (2016).
26. Damasio, A. & Carvalho, G. B. The nature of feelings: evolutionary and neurobiological origins. *Nat. Rev. Neurosci.* **14,** 143–152 (2013).
27. Critchley, H. D. & Harrison, N. A. Visceral influences on brain and behavior. *Neuron* **77,** 624–638 (2013).
28. Barrett, L. F. & Satpute, A. B. Large-scale brain networks in affective and social neuroscience: towards an integrative functional architecture of the brain. *Curr. Opin. Neurobiol.* **23,** 361–372 (2013).
29. Anderson, M. L. *After Phrenology: Neural Reuse and the Interactive Brain* (MIT Press, 2014).
30. Yeo, B. T. *et al.* Functional specialization and flexibility in human association cortex. *Cereb. Cortex* **25,** 3654–3672 (2015).
31. Barbas, H. & Rempel-Clower, N. Cortical structure predicts the pattern of corticocortical connections. *Cereb. Cortex* **7,** 635–646 (1997).
32. Barbas, H. General cortical and special prefrontal connections: principles from structure to function. *Annu. Rev. Neurosci.* **38,** 269–289 (2015).
33. Rempel-Clower, N. L. & Barbas, H. The laminar pattern of connections between prefrontal and anterior temporal cortices in the rhesus monkey is related to cortical structure and function. *Cereb. Cortex* **10,** 851–865 (2000).
34. Medalla, M. & Barbas, H. Specialized prefrontal 'auditory fields': organization of primate prefrontal-temporal pathways. *Front. Neurosci.* **8,** 77 (2014).
35. Medalla, M. & Barbas, H. Diversity of laminar connections linking periarcuate and lateral intraparietal areas depends on cortical structure. *Eur. J. Neurosci.* **23,** 161–179 (2006).
36. Hilgetag, C. C. & Grant, S. Cytoarchitectural differences are a key determinant of laminar projection origins in the visual cortex. *Neuroimage* **51,** 1006–1017 (2010).
37. Goulas, A., Uylings, H. B. & Stiers, P. Mapping the hierarchical layout of the structural network of the macaque prefrontal cortex. *Cereb. Cortex* **24,** 1178–1194 (2014).
38. Bastos, A. M. *et al.* Canonical microcircuits for predictive coding. *Neuron* **76,** 695–711 (2012).
39. Adams, R. A., Stephan, K. E., Brown, H. R., Frith, C. D. & Friston, K. J. The computational anatomy of psychosis. *Front. Psychiatry* **4,** 47 (2013).
40. Shipp, S., Adams, R. A. & Friston, K. J. Reflections on agranular architecture: predictive coding in the motor cortex. *Trends Neurosci.* **36,** 706–716 (2013).
41. Weston, C. S. Another major function of the anterior cingulate cortex: the representation of requirements. *Neurosci. Biobehav. Rev.* **36,** 90–110 (2012).
42. Vogt, B. A. Pain and emotion interactions in subregions of the cingulate gyrus. *Nat. Rev. Neurosci.* **6,** 533–544 (2005).
43. Ongur, D., An, X. & Price, J. L. Prefrontal cortical projections to the hypothalamus in macaque monkeys. *J. Comp. Neurol.* **401,** 480–505 (1998).
44. Vogt, B. A., Vogt, L., Farber, N. B. & Bush, G. Architecture and neurocytology of monkey cingulate gyrus. *J. Comp. Neurol.* **485,** 218–239 (2005).
45. Nieuwenhuys, R. The insular cortex: a review. *Prog. Brain Res.* **195,** 123–163 (2012).
46. Avery, J. A. *et al.* A common gustatory and interoceptive representation in the human mid-insula. *Hum. Brain Mapp.* **36,** 2996–3006 (2015).
47. Hutchison, R. M. & Everling, S. Monkey in the middle: why non-human primates are needed to bridge the gap in resting-state investigations. *Front. Neuroanat.* **6,** 29 (2012).
48. Deco, G., Jirsa, V. K. & McIntosh, A. R. Emerging concepts for the dynamical organization of resting-state activity in the brain. *Nat. Rev. Neurosci.* **12,** 43–56 (2011).
49. Cohen, A. L. *et al.* Defining functional areas in individual human brains using resting functional connectivity MRI. *Neuroimage* **41,** 45–57 (2008).
50. Raichle, M. E. The brain's default mode network. *Annu. Rev. Neurosci.* **38,** 433–447 (2015).
51. Touroutoglou, A., Hollenbeck, M., Dickerson, B. C. & Barrett, L. F. Dissociable large-scale networks anchored in the right anterior insula subserve affective experience and attention. *Neuroimage* **60,** 1947–1958 (2012).
52. Seeley, W. W. *et al.* Dissociable intrinsic connectivity networks for salience processing and executive control. *J. Neurosci.* **27,** 2349–2356 (2007).
53. Dosenbach, N. U., Fair, D. A., Cohen, A. L., Schlaggar, B. L. & Petersen, S. E. A dual-networks architecture of top-down control. *Trends Cogn. Sci.* **12,** 99–105 (2008).
54. Corbetta, M. & Shulman, G. L. Control of goal-directed and stimulus-driven attention in the brain. *Nat. Rev. Neurosci.* **3,** 201–215 (2002).
55. Yeo, B. T. *et al.* The organization of the human cerebral cortex estimated by intrinsic functional connectivity. *J. Neurophysiol.* **106,** 1125–1165 (2011).
56. Nieuwenhuys, R., Voogd, J. & van Huijzen, C. in *The Human Central Nervous System* Ch. 8, 253–279 (Springer, 2008).
57. Brooks, J. C., Faull, O. K., Pattinson, K. T. & Jenkinson, M. Physiological noise in brainstem fMRI. *Front. Hum. Neurosci.* **7,** 623 (2013).
58. Craig, A. D. How do you feel — now? The anterior insula and human awareness. *Nat. Rev. Neurosci.* **10,** 59–70 (2009).
59. Ongur, D. & Price, J. L. The organization of networks within the orbital and medial prefrontal cortex of rats, monkeys and humans. *Cereb. Cortex* **10,** 206–219 (2000).
60. Hoistad, M. & Barbas, H. Sequence of information processing for emotions through pathways linking temporal and insular cortices with the amygdala. *Neuroimage* **40,** 1016–1033 (2008).
61. Lang, P. J., Bradley, M. M. & Cuthbert, B. N. *International Affective Picture System (IAPS): Affective Ratings of Pictures and Instruction Manual* Technical Report A-8 (Univ. of Florida, 2008).
62. Moriguchi, Y. *et al.* Differential hemodynamic response in affective circuitry with aging: an fMRI study of novelty, valence, and arousal. *J. Cogn. Neurosci.* **23,** 1027–1041 (2011).
63. Weierich, M. R., Wright, C. I., Negreira, A., Dickerson, B. C. & Barrett, L. F. Novelty as a dimension in the affective brain. *Neuroimage* **49,** 2871–2878 (2010).
64. Damasio, A. R. *Descartes' Error: Emotion, Reason, and the Human Brain* (Putnam, 1994).
65. Wiens, S., Mezzacappa, E. S. & Katkin, E. S. Heartbeat detection and the experience of emotions. *Cogn. Emot.* **14,** 417–427 (2000).
66. Barrett, L. F., Quigley, K. S., Bliss-Moreau, E. & Aronson, K. R. Interoceptive sensitivity and self-reports of emotional experience. *J. Pers. Soc. Psychol.* **87,** 684–697 (2004).
67. Dunn, B. D. *et al.* Listening to your heart: how interoception shapes emotion experience and intuitive decision making. *Psychol. Sci.* **21,** 1835–1844 (2010).

© 2017 Macmillan Publishers Limited, part of Springer Nature. All rights reserved.

68. Whitehead, W. E., Drescher, V. M., Heiman, P. & Blackwell, B. Relation of heart rate control to heartbeat perception. *Biofeedback Self-Regul.* **2,** 371–392 (1977).
69. Schandry, R. Heart beat perception and emotional experience. *Psychophysiology* **18,** 483–488 (1981).
70. Kleckner, I. R., Wormwood, J. B., Simmons, W. K., Barrett, L. F. & Quigley, K. S. Methodological recommendations for a heartbeat detection-based measure of interoceptive sensitivity. *Psychophysiology* **52,** 1432–1440 (2015).
71. Khalsa, S. S., Rudrauf, D., Feinstein, J. S. & Tranel, D. The pathways of interoceptive awareness. *Nat. Neurosci.* **12,** 1494–1496 (2009).
72. Lindquist, K. A. & Barrett, L. F. A functional architecture of the human brain: emerging insights from the science of emotion. *Trends Cogn. Sci.* **16,** 533–540 (2012).
73. van den Heuvel, M. P. & Sporns, O. Rich-club organization of the human connectome. *J. Neurosci.* **31,** 15775–15786 (2011).
74. McIntosh, A. R. Contexts and catalysts: a resolution of the localization and integration of function in the brain. *Neuroinformatics* **2,** 175–182 (2004).
75. Beissner, F., Schumann, A., Brunn, F., Eisentrager, D. & Bar, K. J. Advances in functional magnetic resonance imaging of the human brainstem. *Neuroimage* **86,** 91–98 (2014).
76. Bar, K. J. *et al.* Functional connectivity and network analysis of midbrain and brainstem nuclei. *Neuroimage* **134,** 53–63 (2016).
77. Edlow, B. L., McNab, J. A., Witzel, T. & Kinney, H. C. The structural connectome of the human central homeostatic network. *Brain Connect.* **6,** 187–200 (2016).
78. Dum, R. P., Levinthal, D. J. & Strick, P. L. Motor, cognitive, and affective areas of the cerebral cortex influence the adrenal medulla. *Proc. Natl Acad. Sci. USA* **113,** 9922–9927 (2016).
79. Blessing, W. W. & Benarroch, E. E. in *The Human Nervous System* (eds Mai, J. K. & Paxinos, G.) 1058–1073 (Academic, 2012).
80. Simmons, W. K. *et al.* Keeping the body in mind: insula functional organization and functional connectivity integrate interoceptive, exteroceptive, and emotional awareness. *Hum. Brain Mapp.* **34,** 2944–2958 (2012).
81. Margulies, D. S. *et al.* Mapping the functional connectivity of anterior cingulate cortex. *Neuroimage* **37,** 579–588 (2007).
82. Bickart, K. C., Dickerson, B. C. & Barrett, L. F. The amygdala as a hub in brain networks that support social life. *Neuropsychologia* **63,** 235–248 (2014).
83. Smith, D. V., Clithero, J. A., Boltuck, S. E. & Huettel, S. A. Functional connectivity with ventromedial prefrontal cortex reflects subjective value for social rewards. *Soc. Cogn. Affect. Neurosci.* **9,** 2017–2025 (2014).
84. van den Heuvel, M. P., Kahn, R. S., Goni, J. & Sporns, O. High-cost, high-capacity backbone for global brain communication. *Proc. Natl Acad. Sci. USA* **109,** 11372–11377 (2012).
85. van den Heuvel, M. P. & Sporns, O. An anatomical substrate for integration among functional networks in human cortex. *J. Neurosci.* **33,** 14489–14500 (2013).
86. Mesulam, M. M. From sensation to cognition. *Brain* **121,** 1013–1052 (1998).
87. Zold, C. L. & Hussain Shuler, M. G. Theta oscillations in visual cortex emerge with experience to convey expected reward time and experienced reward rate. *J. Neurosci.* **35,** 9603–9614 (2015).
88. Satpute, A. B. *et al.* Involvement of sensory regions in affective experience: a meta-analysis. *Front. Psychol.* **6,** 1860 (2015).
89. Vuilleumier, P. How brains beware: neural mechanisms of emotional attention. *Trends Cogn. Sci.* **9,** 585–594 (2005).
90. Allen, M. *et al.* Anterior insula coordinates hierarchical processing of tactile mismatch responses. *Neuroimage* **127,** 34–43 (2016).
91. Sun, F. W. *et al.* Youthful brains in older adults: preserved neuroanatomy in the default mode and salience networks contributes to youthful memory in superaging. *J. Neurosci.* **36,** 9659–9668 (2016).
92. Barrett, L. F. & Bliss-Moreau, E. Affect as a psychological primitive. *Adv. Exp. Soc. Psychol.* **41,** 167–218 (2009).
93. Barrett, L. F. & Russell, J. A. Structure of current affect: controversies and emerging consensus. *Curr. Dir. Psychol. Sci.* **8,** 10–14 (1999).
94. Kuppens, P., Tuerlinckx, F., Russell, J. A. & Barrett, L. F. The relation between valence and arousal in subjective experience. *Psychol. Bull.* **139,** 917–940 (2013).
95. Damasio, A. R. *The Feeling of What Happens: Body and Emotion in the Making of Consciousness* (Houghton Mifflin Harcourt, 1999).
96. Dreyfus, G. & Thompson, E. in *The Cambridge Handbook of Consciousness* (Zelazo, P. D., Moscovitch, M. & Thompson, E.) 89–114 (Cambridge Univ. Press, 2007).
97. Edelman, G. M. & Tononi, G. *A Universe of Consciousness: How Matter Becomes Imagination* (Basic Books, 2000).
98. James, W. *The Principles of Psychology* Vol. 1 (Dover, 1890/2007).
99. Searle, J. R. *The Rediscovery of the Mind* (MIT Press, 1992).
100. Searle, J. R. *Mind: A Brief Introduction* (Oxford Univ. Press, 2004).
101. Wundt, W. *Outlines of Psychology* (Wilhelm Engelmann, 1897).
102. Fodor, J. A. *The Modularity of Mind: An Essay on Faculty Psychology* (MIT Press, 1983).
103. Li, D., Christ, S. E. & Cowan, N. Domain-general and domain-specific functional networks in working memory. *Neuroimage* **102,** 646–656 (2014).
104. Fuster, J. M. *The Module: Crisis of a Paradigm* (Cell, 2000).
105. Kayser, C., Petkov, C. I., Augath, M. & Logothetis, N. K. Functional imaging reveals visual modulation of specific fields in auditory cortex. *J. Neurosci.* **27,** 1824–1835 (2007).
106. Liang, M., Mouraux, A., Hu, L. & Iannetti, G. D. Primary sensory cortices contain distinguishable spatial patterns of activity for each sense. *Nat. Commun.* **4,** 1979 (2013).
107. Edelman, G. M. & Gally, J. A. Degeneracy and complexity in biological systems. *Proc. Natl Acad. Sci. USA* **98,** 13763–13768 (2001).
108. Tong, Y. *et al.* Systemic low-frequency oscillations in bold signal vary with tissue type. *Front. Neurosci.* **10,** 313 (2016).
109. Satpute, A. B. *et al.* Identification of discrete functional subregions of the human periaqueductal gray. *Proc. Natl Acad. Sci. USA* **110,** 17101–17106 (2013).
110. Murphy, K., Birn, R. M., Handwerker, D. A., Jones, T. B. & Bandettini, P. A. The impact of global signal regression on resting state correlations: are anti-correlated networks introduced? *Neuroimage* **44,** 893–905 (2009).
111. Raz, G. *et al.* Functional connectivity dynamics during film viewing reveal common networks for different emotional experiences. *Cogn. Affect. Behav. Neurosci.* **16,** 709–723 (2016).
112. Morrison, S. F. Differential control of sympathetic outflow. *Am. J. Physiol. Regul. Integr. Comp. Physiol.* **281,** R683–698 (2001).
113. Buckner, R. L. The serendipitous discovery of the brain's default network. *Neuroimage* **62,** 1137–1145 (2012).
114. Mesulam, M. The evolving landscape of human cortical connectivity: facts and inferences. *Neuroimage* **62,** 2182–2189 (2012).
115. Hassabis, D. & Maguire, E. A. The construction system of the brain. *Phil. Trans. R. Soc. Lond. B* **364,** 1263–1271 (2009).
116. Power, J. D. *et al.* Functional network organization of the human brain. *Neuron* **72,** 665–678 (2011).
117. Menon, V. & Uddin, L. Q. Saliency, switching, attention and control: a network model of insula function. *Brain Struct. Funct.* **214,** 655–667 (2010).
118. Li, S. S. & McNally, G. P. The conditions that promote fear learning: prediction error and pavlovian fear conditioning. *Neurobiol. Learn. Mem.* **108,** 14–21 (2014).
119. Barrett, L. F. *How Emotions Are Made: The New Science of the Mind and Brain* (Houghton Mifflin Harcourt, 2016).
120. Guidi, M., Huber, L., Lampe, L., Gauthier, C. J. & Moller, H. E. Lamina-dependent calibrated bold response in human primary motor cortex. *Neuroimage* **141,** 250–261 (2016).
121. Crossley, N. A. *et al.* The hubs of the human connectome are generally implicated in the anatomy of brain disorders. *Brain* **137,** 2382–2395 (2014).
122. Goodkind, M. *et al.* Identification of a common neurobiological substrate for mental illness. *JAMA Psychiatry* **72,** 305–315 (2015).
123. Menon, V. Large-scale brain networks and psychopathology: a unifying triple network model. *Trends Cogn. Sci.* **15,** 483–506 (2011).
124. Harshaw, C. Interoceptive dysfunction: toward an integrated framework for understanding somatic and affective disturbance in depression. *Psychol. Bull.* **141,** 311–363 (2015).
125. Paulus, M. P. & Stein, M. B. Interoception in anxiety and depression. *Brain Struct. Funct.* **214,** 451–463 (2010).
126. Naqvi, N. H. & Bechara, A. The insula and drug addiction: an interoceptive view of pleasure, urges, and decision-making. *Brain Struct. Funct.* **214,** 435–450 (2010).
127. Farmer, M. A., Baliki, M. N. & Apkarian, A. V. A dynamic network perspective of chronic pain. *Neurosci. Lett.* **520,** 197–203 (2012).
128. Mayer, E. A. Gut feelings: the emerging biology of gut–brain communication. *Nat. Rev. Neurosci.* **12,** 453–466 (2011).
129. Radley, J., Morilak, D., Viau, V. & Campeau, S. Chronic stress and brain plasticity: mechanisms underlying adaptive and maladaptive changes and implications for stress-related cns disorders. *Neurosci. Biobehav. Rev.* **58,** 79–91 (2015).
130. Gianaros, P. J. & Wager, T. D. Brain–body pathways linking psychological stress and physical health. *Curr. Dir. Psychol. Sci.* **24,** 313–321 (2015).
131. Gefen, T. *et al.* Morphometric and histologic substrates of cingulate integrity in elders with exceptional memory capacity. *J. Neurosci.* **35,** 1781–1791 (2015).
132. Rogalski, E. J. *et al.* Youthful memory capacity in old brains: anatomic and genetic clues from the northwestern superaging project. *J. Cogn. Neurosci.* **25,** 29–36 (2013).

© 2017 Macmillan Publishers Limited, part of Springer Nature. All rights reserved.

133. Angevaren, M., Aufdemkampe, G., Verhaar, H. J., Aleman, A. & Vanhees, L. Physical activity and enhanced fitness to improve cognitive function in older people without known cognitive impairment. *Cochrane Database Syst Rev*. http://dx.doi.org/10.1002/14651858.CD005381.pub3 (2008).
134. Farb, N. *et al.* Interoception, contemplative practice, and health. *Front. Psychol.* **6,** 763 (2015).
135. Tang, Y. Y., Holzel, B. K. & Posner, M. I. The neuroscience of mindfulness meditation. *Nat. Rev. Neurosci.* **16,** 213–225 (2015).
136. Thombs, B. D. *et al.* Prevalence of depression in survivors of acute myocardial infarction. *J. Gen. Intern. Med.* **21,** 30–38 (2006).
137. Moreno-Smith, M., Lutgendorf, S. K. & Sood, A. K. Impact of stress on cancer metastasis. *Future Oncol.* **6,** 1863–1881 (2010).
138. Kolodny, A. *et al.* The prescription opioid and heroin crisis: a public health approach to an epidemic of addiction. *Annu. Rev. Public Health* **36,** 559–574 (2015).
139. Turecki, G. & Brent, D. A. Suicide and suicidal behaviour. *Lancet* **387,** 1227–1239 (2016).
140. Buckner, R. L., Krienen, F. M., Castellanos, A., Diaz, J. C. & Yeo, B. T. The organization of the human cerebellum estimated by intrinsic functional connectivity. *J. Neurophysiol.* **106,** 2322–2345 (2011).
141. Touroutoglou, A., Andreano, J. M., Barrett, L. F. & Dickerson, B. C. Brain network connectivity–behavioral relationships exhibit trait-like properties: evidence from hippocampal connectivity and memory. *Hippocampus* **25,** 1591–1598 (2015).
142. Kramer, J. H. *et al.* NIH EXAMINER: conceptualization and development of an executive function battery. *J. Int. Neuropsychol. Soc.* **20,** 11–19 (2014).
143. Bradley, M. M. & Lang, P. J. Measuring emotion: the self-assessment manikin and the semantic differential. *J. Behav. Ther. Exp. Psychiatry* **25,** 49–59 (1994).
144. Bohus, B. *et al.* The neurobiology of the central nucleus of the amygdala in relation to neuroendocrine and autonomic outflow. *Prog. Brain Res.* **107,** 447–460 (1996).
145. Mufson, E. J., Mesulam, M. M. & Pandya, D. N. Insular interconnections with the amygdala in rhesus monkey. *Neuroscience* **6,** 1231–1248 (1981).
146. Mufson, E. J. & Mesulam, M. M. Insula of the old world monkey. II: afferent cortical input and comments on the claustrum. *J. Comp. Neurol.* **212,** 23–37 (1982).
147. Ghashghaei, H. T., Hilgetag, C. C. & Barbas, H. Sequence of information processing for emotions based on the anatomic dialogue between prefrontal cortex and amygdala. *Neuroimage* **34,** 905–923 (2007).
148. Jo, H. J. *et al.* Effective preprocessing procedures virtually eliminate distance-dependent motion artifacts in resting state fMRI. *J. Appl. Math.* **2013,** 935154 (2013).
149. Power, J. D., Barnes, K. A., Snyder, A. Z., Schlaggar, B. L. & Petersen, S. E. Spurious but systematic correlations in functional connectivity mri networks arise from subject motion. *Neuroimage* **59,** 2142–2154 (2012).
150. Tucholka, A., Fritsch, V., Poline, J. B. & Thirion, B. An empirical comparison of surface-based and volume-based group studies in neuroimaging. *Neuroimage* **63,** 1443–1453 (2012).
151. Cronbach, L. J., Rajaratnam, N. & Gleser, G. C. Theory of generalizability: a liberalization of reliability theory. *Br. J. Stat. Psychol.* **16,** 137–163 (1963).
152. Boucsein, W. *et al.* Publication recommendations for electrodermal measurements. *Psychophysiology* **49,** 1017–1034 (2012).
153. Schell, A. M., Dawson, M. E. & Filion, D. L. Psychophysiological correlates of electrodermal lability. *Psychophysiology* **25,** 619–632 (1988).
154. Xia, C., Touroutoglou, A., Quigley, K. S., Barrett, L. F. & Dickerson, B. C. Salience network connectivity modulates skin conductance responses in predicting arousal experience. *J. Cogn. Neurosci.* http://dx.doi.org/10.1162/jocn_a_01087 (2016).
155. Fredrikson, M. *et al.* Functional neuroanatomical correlates of electrodermal activity: a positron emission tomographic study. *Psychophysiology* **35,** 179–185 (1998).
156. Morecraft, R. J. *et al.* Cytoarchitecture and cortical connections of the anterior cingulate and adjacent somatomotor fields in the rhesus monkey. *Brain Res. Bull.* **87,** 457–497 (2012).
157. Mesulam, M. M. & Mufson, E. J. Insula of the old world monkey. III: efferent cortical output and comments on function. *J. Comp. Neurol.* **212,** 38–52 (1982).
158. Cavdar, S. *et al.* The afferent connections of the posterior hypothalamic nucleus in the rat using horseradish peroxidase. *J. Anat.* **198,** 463–472 (2001).
159. An, X., Bandler, R., Ongur, D. & Price, J. L. Prefrontal cortical projections to longitudinal columns in the midbrain periaqueductal gray in macaque monkeys. *J. Comp. Neurol.* **401,** 455–479 (1998).
160. Saper, C. B. Reciprocal parabrachial–cortical connections in the rat. *Brain Res.* **242,** 33–40 (1982).
161. Saper, C. B. Convergence of autonomic and limbic connections in the insular cortex of the rat. *J. Comp. Neurol.* **210,** 163–173 (1982).
162. Fudge, J. L., Breitbart, M. A., Danish, M. & Pannoni, V. Insular and gustatory inputs to the caudal ventral striatum in primates. *J. Comp. Neurol.* **490,** 101–118 (2005).
163. Carmichael, S. T. & Price, J. L. Connectional networks within the orbital and medial prefrontal cortex of macaque monkeys. *J. Comp. Neurol.* **371,** 179–207 (1996).
164. Aggleton, J. P., Burton, M. J. & Passingham, R. E. Cortical and subcortical afferents to the amygdala of the rhesus monkey (*Macaca mulatta*). *Brain Res.* **190,** 347–368 (1980).
165. Stefanacci, L. & Amaral, D. G. Some observations on cortical inputs to the macaque monkey amygdala: an anterograde tracing study. *J. Comp. Neurol.* **451,** 301–323 (2002).
166. Chikama, M., McFarland, N. R., Amaral, D. G. & Haber, S. N. Insular cortical projections to functional regions of the striatum correlate with cortical cytoarchitectonic organization in the primate. *J. Neurosci.* **17,** 9686–9705 (1997).
167. Chiba, T., Kayahara, T. & Nakano, K. Efferent projections of infralimbic and prelimbic areas of the medial prefrontal cortex in the Japanese monkey, *Macaca fuscata*. *Brain Res.* **888,** 83–101 (2001).
168. Vogt, B. A. & Pandya, D. N. Cingulate cortex of the rhesus monkey. II. Cortical afferents. *J. Comp. Neurol.* **262,** 271–289 (1987).
169. Rempel-Clower, N. L. & Barbas, H. Topographic organization of connections between the hypothalamus and prefrontal cortex in the rhesus monkey. *J. Comp. Neurol.* **398,** 393–419 (1998).
170. Freedman, L. J., Insel, T. R. & Smith, Y. Subcortical projections of area 25 (subgenual cortex) of the macaque monkey. *J. Comp. Neurol.* **421,** 172–188 (2000).
171. Terreberry, R. R. & Neafsey, E. J. Rat medial frontal cortex: a visceral motor region with a direct projection to the solitary nucleus. *Brain Res.* **278,** 245–249 (1983).
172. van der Kooy, D., McGinty, J. F., Koda, L. Y., Gerfen, C. R. & Bloom, F. E. Visceral cortex: a direct connection from prefrontal cortex to the solitary nucleus in rat. *Neurosci. Lett.* **33,** 123–127 (1982).
173. Room, P., Russchen, F. T., Groenewegen, H. J. & Lohman, A. H. Efferent connections of the prelimbic (area 32) and the infralimbic (area 25) cortices: an anterograde tracing study in the cat. *J. Comp. Neurol.* **242,** 40–55 (1985).
174. Pandya, D. N., Van Hoesen, G. W. & Mesulam, M. M. Efferent connections of the cingulate gyrus in the rhesus monkey. *Exp. Brain Res.* **42,** 319–330 (1981).
175. Vogt, B. A. & Palomero-Gallagher, N. in *The Human Nervous System* (eds Mai, J. K. & Paxinos, G.) Ch. 25, 943–987 (Academic, 2012).
176. Haber, S. N., Kim, K. S., Mailly, P. & Calzavara, R. Reward-related cortical inputs define a large striatal region in primates that interface with associative cortical connections, providing a substrate for incentive-based learning. *J. Neurosci.* **26,** 8368–8376 (2006).
177. Price, J. L. & Amaral, D. G. An autoradiographic study of the projections of the central nucleus of the monkey amygdala. *J. Neurosci.* **1,** 1242–1259 (1981).
178. Fudge, J. L., Kunishio, K., Walsh, P., Richard, C. & Haber, S. N. Amygdaloid projections to ventromedial striatal subterritories in the primate. *Neuroscience* **110,** 257–275 (2002).
179. Morecraft, R. J. & Van Hoesen, G. W. Convergence of limbic input to the cingulate motor cortex in the rhesus monkey. *Brain Res. Bull.* **45,** 209–232 (1998).
180. Saleem, K. S., Kondo, H. & Price, J. L. Complementary circuits connecting the orbital and medial prefrontal networks with the temporal, insular, and opercular cortex in the macaque monkey. *J. Comp. Neurol.* **506,** 659–693 (2008).
181. Barbas, H., Ghashghaei, H., Dombrowski, S. M. & Rempel-Clower, N. L. Medial prefrontal cortices are unified by common connections with superior temporal cortices and distinguished by input from memory-related areas in the rhesus monkey. *J. Comp. Neurol.* **410,** 343–367 (1999).
182. Ongur, D., Ferry, A. T. & Price, J. L. Architectonic subdivision of the human orbital and medial prefrontal cortex. *J. Comp. Neurol.* **460,** 425–449 (2003).
183. Ghaziri, J. *et al.* The corticocortical structural connectivity of the human insula. *Cereb. Cortex* http://dx.doi.org/10.1093/cercor/bhv308 (2015).
184. Wiech, K., Jbabdi, S., Lin, C. S., Andersson, J. & Tracey, I. Differential structural and resting state connectivity between insular subdivisions and other pain-related brain regions. *Pain* **155,** 2047–2055 (2014).
185. Gianaros, P. J. & Sheu, L. K. A review of neuroimaging studies of stressor-evoked blood pressure reactivity: emerging evidence for a brain-body pathway to coronary heart disease risk. *Neuroimage* **47,** 922–936 (2009).
186. Kurth, F., Zilles, K., Fox, P. T., Laird, A. R. & Eickhoff, S. B. A link between the systems: functional differentiation and integration within the human insula revealed by meta-analysis. *Brain Struct. Funct.* **214,** 519–534 (2010).

© 2017 Macmillan Publishers Limited, part of Springer Nature. All rights reserved.

187. Gianaros, P. J. *et al.* An inflammatory pathway links atherosclerotic cardiovascular disease risk to neural activity evoked by the cognitive regulation of emotion. *Biol. Psychiatry* **75,** 738–745 (2014).
188. Wager, T. D. *et al.* Brain mediators of cardiovascular responses to social threat. Part I: reciprocal dorsal and ventral sub-regions of the medial prefrontal cortex and heart-rate reactivity. *Neuroimage* **47,** 821–835 (2009).
189. Harper, R. M. *et al.* fMRI responses to cold pressor challenges in control and obstructive sleep apnea subjects. *J. Appl. Physiol.* **94,** 1583–1595 (2003).
190. Gianaros, P. J. *et al.* Individual differences in stressor-evoked blood pressure reactivity vary with activation, volume, and functional connectivity of the amygdala. *J. Neurosci.* **28,** 990–999 (2008).
191. Zilles, K. & Amunts, K. in *The Human Nervous System* (eds Mai, J. K. & Paxinos G.) Ch. 23, 836–895 (Elsevier, 2012).
192. Petrides, M. & Pandya, D. N. in *The Human Nervous System* (eds Mai, J. K. & Paxinos, G.) Ch. 26, 988–1011 (Elsevier, 2012).
193. Barbas, H. Specialized elements of orbitofrontal cortex in primates. *Ann. NY Acad. Sci.* **1121,** 10–32 (2007).
194. Mesulam, M. M. & Mufson, E. J. Insula of the old world monkey. I. Architectonics in the insulo-orbito-temporal component of the paralimbic brain. *J. Comp. Neurol.* **212,** 1–22 (1982).
195. Yarkoni, T. Big correlations in little studies: inflated fMRI correlations reflect low statistical power — commentary on Vul *et al.* (2009). *Persp. Psychol. Sci.* **4,** 294–298 (2009).
196. Wilson-Mendenhall, C. D., Barrett, L. F., Simmons, W. K. & Barsalou, L. W. Grounding emotion in situated conceptualization. *Neuropsychologia* **49,** 1105–1127 (2011).
197. Wilson-Mendenhall, C. D., Barrett, L. F. & Barsalou, L. W. Variety in emotional life: within-category typicality of emotional experiences is associated with neural activity in large-scale brain networks. *Soc. Cogn. Affect. Neurosci.* **10,** 62–71 (2015).
198. Kober, H. *et al.* Functional grouping and cortical-subcortical interactions in emotion: A meta-analysis of neuroimaging studies. *Neuroimage* **42,** 998–1031 (2008).
199. Skerry, A. E. & Saxe, R. Neural representations of emotion are organized around abstract event features. *Curr. Biol.* **25,** 1945–1954 (2015).
200. Clithero, J. A. & Rangel, A. Informatic parcellation of the network involved in the computation of subjective value. *Soc. Cogn. Affect. Neurosci.* **9,** 1289–1302 (2014).
201. Bickart, K. C., Hollenbeck, M. C., Barrett, L. F. & Dickerson, B. C. Intrinsic amygdala-cortical functional connectivity predicts social network size in humans. *J. Neurosci.* **32,** 14729–14741 (2012).
202. Baliki, M. N., Mansour, A. R., Baria, A. T. & Apkarian, A. V. Functional reorganization of the default mode network across chronic pain conditions. *PLoS ONE* **9,** e106133 (2014).
203. Schurz, M., Radua, J., Aichhorn, M., Richlan, F. & Perner, J. Fractionating theory of mind: a meta-analysis of functional brain imaging studies. *Neurosci. Biobehav. Rev.* **42,** 9–34 (2014).
204. Morelli, S. A. & Lieberman, M. D. The role of automaticity and attention in neural processes underlying empathy for happiness, sadness, and anxiety. *Front. Hum. Neurosci.* **7,** 160 (2013).
205. Chiong, W. *et al.* The salience network causally influences default mode network activity during moral reasoning. *Brain* **136,** 1929–1941 (2013).
206. Liu, X., Hairston, J., Schrier, M. & Fan, J. Common and distinct networks underlying reward valence and processing stages: a meta-analysis of functional neuroimaging studies. *Neurosci. Biobehav. Rev.* **35,** 1219–1236 (2011).
207. Engelmann, J. M. *et al.* Neural substrates of smoking cue reactivity: a meta-analysis of fMRI studies. *Neuroimage* **60,** 252–262 (2012).
208. Schacter, D. L. & Addis, D. R. The cognitive neuroscience of constructive memory: remembering the past and imagining the future. *Phil. Trans. R. Soc. Lond. B* **362,** 773–786 (2007).
209. Bar, M., Aminoff, E., Mason, M. & Fenske, M. The units of thought. *Hippocampus* **17,** 420–428 (2007).
210. Fernandino, L. *et al.* Concept representation reflects multimodal abstraction: A framework for embodied semantics. *Cereb. Cortex* **26,** 2018–2034 (2016).
211. Touroutoglou, A., Lindquist, K. A., Dickerson, B. C. & Barrett, L. F. Intrinsic connectivity in the human brain does not reveal networks for 'basic' emotions. *Soc. Cogn. Affect. Neurosci.* **10,** 1257–1265 (2015).
212. Dhanjal, N. S. & Wise, R. J. Frontoparietal cognitive control of verbal memory recall in alzheimer's disease. *Ann. Neurol.* **76,** 241–251 (2014).
213. Dosenbach, N. U. *et al.* Distinct brain networks for adaptive and stable task control in humans. *Proc. Natl Acad. Sci. USA* **104,** 11073–11078 (2007).
214. Ansell, E. B., Rando, K., Tuit, K., Guarnaccia, J. & Sinha, R. Cumulative adversity and smaller gray matter volume in medial prefrontal, anterior cingulate, and insula regions. *Biol. Psychiatry* **72,** 57–64 (2012).
215. Caseras, X. *et al.* Anatomical and functional overlap within the insula and anterior cingulate cortex during interoception and phobic symptom provocation. *Hum. Brain Mapp.* **34,** 1220–1229 (2013).
216. Wolf, D. H. *et al.* Striatal intrinsic reinforcement signals during recognition memory: relationship to response bias and dysregulation in schizophrenia. *Front. Behav. Neurosci.* **5,** 81 (2011).
217. Grady, C. L., Luk, G., Craik, F. I. & Bialystok, E. Brain network activity in monolingual and bilingual older adults. *Neuropsychologia* **66,** 170–181 (2015).
218. Derbyshire, S. W., Whalley, M. G., Stenger, V. A. & Oakley, D. A. Cerebral activation during hypnotically induced and imagined pain. *Neuroimage* **23,** 392–401 (2004).
219. Feldstein Ewing, S. W., Filbey, F. M., Sabbineni, A., Chandler, L. D. & Hutchison, K. E. How psychosocial alcohol interventions work: a preliminary look at what fMRI can tell us. *Alcohol. Clin. Exp. Res.* **35,** 643–651 (2011).
220. Singer, T. *et al.* Empathy for pain involves the affective but not sensory components of pain. *Science* **303,** 1157–1162 (2004).
221. Kirk, U., Downar, J. & Montague, P. R. Interoception drives increased rational decision-making in meditators playing the ultimatum game. *Front. Neurosci.* **5,** 49 (2011).
222. FitzGerald, T. H., Schwartenbeck, P. & Dolan, R. J. Reward-related activity in ventral striatum is action contingent and modulated by behavioral relevance. *J. Neurosci.* **34,** 1271–1279 (2014).
223. Fernandino, L., Humphries, C. J., Conant, L., Seidenberg, M. S. & Binder, J. R. Heteromodal cortical areas encode sensory-motor features of word meaning. *J. Neurosci.* **36,** 9763–9769 (2016).
224. Hermans, E. J. *et al.* Stress-related noradrenergic activity prompts large-scale neural network reconfiguration. *Science* **334,** 1151–1153 (2011).
225. Clark-Polner, E., Wager, T. D., Satpute, A. B. & Barrett, L. F. in *The Handbook of Emotion* (eds Barrett, L. F., Lewis, M. & Haviland-Jones, J. M.) 146–165 (Guilford Press, 2016).

Acknowledgements

We thank M. A. Garcia-Cabezas for comments and advice on neuroanatomy, and H. Evrard for discussions on anatomical connectivity. This research was supported by funds from the National Institutes on Aging (R01 AG030311) to L.F.B. and B.C.D., the US Army Research Institute for the Behavioral and Social Sciences Contracts (W5J9CQ-11-C-0046 and W5J9CQ-12-C-0049) to L.F.B., the National Cancer Institute (U01 CA193632) to L.F.B., the National Institute of Mental Health Ruth L. Kirschstein National Research Service Award (F32MH096533) to I.R.K., the National Cancer Institute (UG1 CA189961 and R25 CA102618) to support I.R.K., the National Institutes of Mental Health (K01MH096175-01) and Oklahoma Tobacco Research Center grants to W.K.S., a Fyssen Foundation postdoctoral fellowship and Alicia Koplowitz Foundation short-term fellowship to L.C. and the Fonds de recherche sante Quebec fellowship award to C.X. The views, opinions and findings contained in this paper are those of the authors and shall not be construed as an official Department of the Army position, policy or decision, unless so designated by other documents. The funders had no role in study design, data collection and analysis, decision to publish or preparation of the manuscript.

Author contributions

The study was designed and analysed by all the authors, and the manuscript was written by I.R.K. and L.F.B. with comments and edits from other authors.

Additional information

Supplementary information is available for this paper.

Reprints and permissions information is available at www.nature.com/reprints.

Correspondence and requests for materials should be addressed to I.R.K. or L.F.B.

How to cite this article: Kleckner, I. R. *et al.* Evidence for a large-scale brain system supporting allostasis and interoception in humans. *Nat. Hum. Behav.* **1,** 0069 (2017).

Publisher's note: Springer Nature remains neutral with regard to jurisdictional claims in published maps and institutional affiliations.

Competing interests

The authors declare no competing interests.

© 2017 Macmillan Publishers Limited, part of Springer Nature. All rights reserved.